frontiers | Frontiers in Environmental Archaeology

TYPE Original Research
PUBLISHED 24 November 2025
DOI 10.3389/fearc.2025.1631639

OPEN ACCESS

EDITED BY
Cristina Marilin Calo,
Universidad Nacional de Córdoba, Argentina

REVIEWED BY
Mario Alejandro Caria,
Universidad Nacional de Tucumán, Argentina
Julián Mignino,
CONICET Cordoba, Argentina

*CORRESPONDENCE
Kelly Brandão
✉ kellybrand@gmail.com

RECEIVED 20 May 2025
ACCEPTED 06 October 2025
PUBLISHED 24 November 2025

CITATION
Brandão K, Furquim L, Cangussu D, Strauss A, Mendes dos Santos G, Neves EG and Villagran XS (2025) Multidimensional analysis of indigenous bread from the Brazilian Amazon. *Front. Environ. Archaeol.* 4:1631639. doi: 10.3389/fearc.2025.1631639

Multidimensional analysis of indigenous bread from the Brazilian Amazon

Kelly Brandão[1,2,3]*, Laura Furquim[1,2,3,4,5,6], Daniel Cangussu[7,8], André Strauss[9], Gilton Mendes dos Santos[6], Eduardo Goes Neves[2] and Ximena S. Villagran[1]

[1]Microarchaeology Laboratory, Museum of Archaeology and Ethnology, University of São Paulo, São Paulo, Brazil, [2]Laboratory of Archaeology of the Tropics, Museum of Archaeology and Ethnology, University of São Paulo, São Paulo, Brazil, [3]Archaeology Research Group, Mamirauá Institute for Sustainable Development, Tefé, Brazil, [4]isoTROPIC Research Group, Max Planck Institute of Geoanthropology, Jena, Germany, [5]Department of Archaeology, Max Planck Institute of Geoanthropology, Jena, Germany, [6]Federal University of the Amazonas, Nucleus for Indigenous Amazon Studies, Manaus, Brazil, [7]Madeira Ethno-Environmental Protection Front/FUNAI - National Foundation for Indigenous Peoples, Rondonia, Brazil, [8]Ecologia, Conservação e Manejo da Vida Silvestre - Federal University of Minas Gerais, Belo Horizonte, Brazil, [9]Laboratory of Environmental and Evolutionary Archaeology and Anthropology, Museum of Archaeology and Ethnology, University of São Paulo, São Paulo, Brazil

The Indigenous bread of the Amazon is an ancient food technology, with records dating back at least to 1,200 AD. This food technology survived the colonial period and was continuously produced by Amazonian Indigenous people until the 20th century. Accounts of these breads can be found in chronicles, travelers' records, and the oral traditions passed down by forest peoples. Previous studies rejected the oral history of different indigenous peoples and classified bread as a new species of fungus with a large mycelium. Recent research has reshaped this perspective by identifying a diversity of ingredients and production processes. These new insights reveal different recipes incorporating corn, chili pepper, palm fruits, mairá potato, and other tubers, while highlighting techniques such as fermentation and smoking. This study characterizes indigenous bread using a geo and microarchaeological approach including analytical imaging methods (petrography, stereoscopic mosaic, and micro-computed tomography–micro-CT), which were combined with Fourier-transform infrared spectroscopy (FTIR). Multidimensional analyses identified two distinct bread microstructures: massive and spongy. Additionally, specific manufacturing characteristics were detailed, such as wrapping the bread in organic matter (e.g., leaves), for the massive bread, and in clay, for the spongy bread. Smoking was also used to create a hardened crust on the surface while preserving a soft interior. Analyses also revealed that massive bread contains clay, and clay consumption has been widely described in travelers' accounts and oral traditions in the Amazon. This study contributes to the efforts of archaeobotanical research in understanding the ancient food technology of Amazonian people.

KEYWORDS

Amazonian archaeology, bread production, foodways, ancient technology, forest food, Micro-CT, petrography, FTIR

1 Introduction

In recent decades, archaeobotanical studies have gained prominence in the tropics as a key approach to understanding the lifestyles of past Indigenous populations in the Amazon. The culinary technologies developed by Indigenous people reflect the long lasting landscape legacies (Levis et al., 2017, 2018), including cultural niche creation and biodiversity increase through management and domestication practices (Clement et al., 2015; Stokes et al., 2025). Many of the food technologies developed by Indigenous peoples persist in the daily lives of forest communities, transmitted through oral traditions. Others have been transformed or lost over time, particularly as a result of the period of European colonization (Crosby, 2003) and the consequent process of genetic erosion of local populations due to the transmission of diseases and processes of extermination of different indigenous people por erosao genetica, such as some species of cassava (*Manihot esculenta*) and native cotton (*Gossypium barbadense*) (Humphreys et al., 2019).

Indigenous bread (referred to as "*pão de índio*" in Portuguese) is commonly found buried in various Amazonian environments, including archaeological sites, orchards, and pathways. It is described by Indigenous and Riverine peoples as an ancestral reserve food, capable of being consumed long after its preparation. Indeed, while this technology and recipe no longer exist in the culinary repertoire of contemporary communities, some few people still know where ancient breads are buried and eat them (personal communication described in dos Santos et al., 2021).

The use of the word "bread" to refer to this type of food is closely tied to the European invasion and the descriptions provided by travelers, missionaries, and naturalists, particularly during the 19th and 20th centuries. Indigenous peoples have a complex set of categories and names to describe their foods, some of them recalling flatbreads and loaves of bread, such as *beijus*, *marapatás*, *paparutos,* and many others (França and Fontes, 2022), some of which can be ingredients in the long process of producing part of the certain fermented beverages, as *caxiri*.

In the 1980s, mycological studies classified two of these bread as fungal, interpreting as a large mycelium, specifically from the genus *Pachyma Fr.*, *Polyporus indigenus* (da Silva Araujo and de Sousa, 1978; Aguiar and de Sousa, 1981); the hypothesis about fungal origins was later supported by additional studies (Santos et al., 2014). However, recent research using multi-analytical approaches identified starch grains with physical damage related to milling and baking inside the bread, refuting the hypothesis that they were fungal masses (dos Santos et al., 2021; Furquim, 2024). Studies confirm this bread is a food technology made from plant biomass, yet the specific processes of its preparation and consumption are only beginning to be understood (Furquim, 2024). It was suggested that the archaeological Indigenous bread was a food storage technology largely used during periods of food insecurity or conflicts between social groups, besides being consumed during travels, hunting trips, or long journeys (dos Santos et al., 2021).

The importance of the fermentation of foods and beverages to Amazonian Indigenous foodways is acknowledged in many ethnohistoric and ethnographic studies and plays a central role in ceremonial feasts or daily food consumption (for an extensive revision on the subject see Furquim, 2024; Barghini, 2020, 2022; Perrone-Moisés, 2015; de Oliveira, 2012). A variety of strategies for fermentation are described, including the burial of pulps made of roots, nuts, and fruit seeds in underground pits for specific periods up to 1 year, as preparation for fermented recipes of beijus, pulps, and beverages (França, 2024). In the Upper Negro River basin fruits and seeds of species such as umari (*Poraqueiba sericea Tulasne*), uaçu (*Monopteryx uaucu*), and palm trees like pupunha (*Bactris gasipaes*) and buriti (*Mauritia flexuosa*), as well as roots like cassava and yam (*Dioscorea*), are commonly utilized in these processes (França and Fontes, 2022; França, 2024). These practices underscore the deep ecological and cultural knowledge embedded in Amazonian food systems (dos Santos et al., 2021).

This study focuses on image analysis of Indigenous bread (its structural and compositional characteristics) to advance our understanding of the technology involved in its production. We used a geoarchaeological and microarchaeological approach combining imaging techniques (petrography, stereoscopic mosaic, and micro-CT) with infrared spectroscopy (FTIR). Different imaging techniques allow the observation of materials and structures at various scales and spatial resolutions, thus refining the investigation of properties that are not visible to the naked eye and clarifying the relationships between biomass components. The combination of various imaging techniques provides insights into the technology involved in the entire operational sequence of bread production, the components, manufacturing techniques, and post-depositional alterations. The samples analyzed in this study are part of the collection curated by Laura Furquim, located in the Museum of Archaeology and Ethnology of the University of São Paulo, Amazon Museum, Archaeology Laboratory of the University of Amazonas, and Goeldi Museum (Furquim, 2024), with archaeological, ethnographic, and fortuitously in the fields of traditional communities found specimens. The main objective of these analyses is to characterize the different fabrics and identify possible fermentation bubbles.

2 Methods

The samples analyzed in this study were examined across multiple scales by combining micro-CT imaging, stereoscopic mosaics from macro fragments samples, and petrographic thin sections (Table 1). These methods were further complemented by FTIR spectroscopy, which refined the overall analysis. To perform multi-scalar image analyses, fragments from six breads with distinct macroscopic characteristics were examined. Four of these fragments were prepared for petrographic analysis and stereoscopic mosaics, while all six were analyzed using microtomography. For FTIR spectroscopy, 16 samples were collected from the approximate center of the bread loaves and five from the crust.

Based on the survey of 44 samples conducted by Furquim in different institutions in Brazil (Furquim, 2024), the analyses were carried out according to the type of material available: imaging analyses on samples from which fragments could be collected, and FTIR analyses on samples from which powdered, and fragment material could be obtained.

10.3389/fearc.2025.1631639

TABLE 1 Samples (Indigenous Breads [IB##] and modern comparative cassava flour) and methods applied in this research.

Sample's code	Provenance	Stereo/Microscope analyses		Micro-CT	FTIR		
		Mosaic	Petrography		Central area	Crust area	Other elements
IB01	Jacareúba-Katawixi	x	x	x	x	x	x
IB03	AM-IR-53 Lago do Testa				x		
IB04	ABC – Ramal Manacapuru				x		
IB05	Ramal Manacapuru				x		
IB06	ABC – Ramal Manacapuru				x		
IB07	Fazenda Águas Claras				x		
IB08	Presidente Figueiredo	x	x	x	x	x	x
IB09	TI Kaxinawa (Acre)	x	x	x	x	x	x
IB10	Santarém				x		
IB11	Presidente Figueiredo				x		
IB12	Whitout Provenence (INPA)				x		
IB13	Whitout Provenence (INPA)				x		
IB14	Whitout Provenence (INPA)				x		
IB16	Rio Jacaré (AM)	x	x	x	x	x	
IB42	Tapauá (AM), TI São João (Apurinã)			x	x	x	
IB44	Padaria Rio Paciá			x	x		
YFS	Yellow Cassava Flour - Santarém		x		x		
WFS	White Cassava Flour- Santarém		x		x		
TFS	Tapioca Flour- Santarém		x		x		
YFT	Yellow Cassava Flour- Tefé		x		x		
WFB	White Cassava Flour- Belém		x		x		

Additionally, five cassava flour samples were subjected to petrographic and FTIR analyses for comparative fiber processing purposes. The choice of cassava flour was due to the identification of cassava starch in some breads and because it is the type of flour with indigenous origins, very common in Brazil and with different known processing methods.

2.1 Micro-CT

Six fragments of Indigenous breads (IB01, IB08, IB09, IB16, IB42, and IB44) were scanned using Micro-CT. This technique enables the creation of high-solution three-dimensional images of the material's internal structure, facilitates the observation of external surface marks, and allows detailed volumetric analyses. The scans were carried out using the ZEISS Xradia Versa XRM-510 (micro-CT). For image reconstruction, Scout and Scan-Control System Reconstructor were employed, and the analyses were performed with Avizo 8.1. The use of microtomography complements the analysis of the slides, allowing for the observation of void dispersions in three dimensions and the detailed examination of features such as the bread crust. The specific parameters of each scan are detailed in Table 2.

Micro-CT analyses allow us to compare the material densities within each sample. The air density (observed in darker colors) served as a reference for the least dense material, while the

TABLE 2 Scan conditions of the bread loaf fragments.

Sample ID	IB01	IB08	IB09	IB16	IB42	IB44
Objective	0.4 x	0.4 x	0.4 x	0.4 x	0.4 x	0.4 x
Source settings	100 kv/9w	160 kv/10W	100 kv/9w	100 kv/9w	160 kv/10W	140 kv/10W
Pixel size (μm)	28.83	17.26	55.47	28.83	24.47	28.73
Number of views	1,000	1,000	1,000	1,000	1,000	1,200
Time per view (sec)	1	1,3	1	1	1,2	1,2
Resol. Detector	Bin 2	Bin 2	Bin 2	Bin 2	Bin 2	Bin 2
Filter	Air	Air	Air	Air	Air	Air

bright areas in the scans represent materials with higher density. This approach relies on the principle that X-ray attenuation is directly proportional to the density of the material being scanned, generating a grayscale attenuation map. These maps enable the differentiation of components within heterogeneous samples and provide a framework for identifying specific materials or inclusions.

2.2 Petrographic and mosaic analysis

Observation of the material through thin sections reveals the matrix as it is, functioning as a detailed microscopic "photograph" of the Indigenous bread. This method allows the description of relationships between different components and the microstructure, as well as the analysis of alteration processes affecting the loaves of bread. Since no specific guidelines exist for this type of material, the descriptions and interpretation adhered to the standards of soil micromorphology (Bullock et al., 1985; Stoops, 2021) and ceramic petrography (Quinn, 2022, 2013). This dual approach was essential due to the material's unique characteristics, which involve dough manipulation, combining organic and inorganic components, undergoing thermal transformations, and exhibiting features indicative of clay illuviation, such as coatings and infillings.

Mosaics capture the visual features of bread sample fragments under a stereoscope using oblique incident light. While some characteristics are visible to the naked eye, others require magnification or additional imaging techniques. Therefore, this method is integrated with other image analyses to explore various properties and behaviors of the elements that compose the samples. Mosaic images of hand samples were made with the Carl Zeiss Stereomicroscope–Stemi SV.11 in the Sedimentary Petrography Laboratory (LABPETRO) Geosciences Institute (USP).

The thin sections were prepared following the impregnation protocol established by the Microarchaeology Laboratory at the Museum of Archaeology and Ethnology (USP). The samples were dried at 40 °C for 72 h and impregnated with a mixture of Crystal Polyester Resin, Styrene Monomer, and catalyst. After complete curing, the samples were cut, and the thin sections were made with dimensions of 5×7 cm and a thickness of 30 μm. Thin sections were analyzed using the Leica D2700P and Carl Zeiss Axioplan 2 petrographic microscope, the Leica S9i stereomicroscope. Petrographic analyses were performed under transmitted, reflected, and fluorescent light. High-resolution scanning of the thin section was carried out using the Epson Perfection V800 photo scanner.

2.3 Comparative cassava flours

To support the interpretation and discussion of the data from the analyzed Indigenous bread loaves, microscope slides were prepared and FTIR spectra were collected from five samples of cassava flour with different culinary and physical characteristics, originating from three Amazonian cities: Tefé (Amazonas), Santarém, and Belém (Pará). Cassava was selected as the subject of study because it is one of the most frequently identified starches in Amazon Indigenous bread samples by Furquim (2024) and different forms of processing are readily accessible for sampling.

This experiment aimed to locate and photograph cassava fiber fragments, compare them with microscopic fibers found in the bread samples, and expand the FTIR database. The samples were ground using an agate mortar and pestle, which was decontaminated between samples with a diluted acid solution and isopropyl alcohol. The microscope slides were prepared using less than one gram of homogenized flour covered with a 1:1 mixture of glycerin and water and covered with a cover slip. For the FTIR analysis, the samples were ground until they reached a very fine sand-to-silt texture, and spectra were collected following the procedure described in Section 2.4.

2.4 FTIR

FTIR spectroscopy in archaeology is a well-established method for analyzing organic and inorganic materials and identifying burned materials at different temperatures (Berna et al., 2007; Weiner, 2010; Villagran et al., 2017). For this study, samples were collected from the center of all 16 Indigenous breads and 5 samples from the crust of these specimens that macroscopically demonstrated an external layer that differed from the internal ones. FTIR analyses were performed using a Cary 630 spectrometer (Agilent Technologies) equipped with KBr optics, enabling the acquisition of spectra via attenuated total reflectance (ATR) with 32 scans in the spectral range of 4,000–400 cm^{-1}. The samples were scraped and finely ground using an agate mortar and pestle, which was cleaned with a diluted acid solution and isopropyl alcohol between samples to avoid contamination.

FTIR analysis was used to identify organic and inorganic components in the samples and to investigate thermal alterations and compositional differences. This method was supported by results of the analyses of images, starch grains, and lipids conducted by Furquim (2024), which showed that the bread samples are

complexes. To address this, the results of previous analyses were combined with experiments using cassava flour as a reference material and literature available.

3 Results

Macroscopic and microscope observations show differences among most of the breads, which were categorized into two groups: those with massive and those with spongy mass structures. However, the category of internal structure of some samples was not identified.

3.1 Micro-CT

Micro-CT analyses revealed that the bread samples can be categorized into at least two distinct structures: Structure 1 (S1) and Structure 2 (S2). S1, represented by samples IB01, IB08, IB09, and IB44, (Figure 1) is characterized by a matrix with gradual grayscale variations, reflecting random density differences. Additionally, it features a coarse fraction with distinct density variations. In contrast, S2, identified in samples IB16 and IB44 (Figure 2), displays regions of low (dark gray) and high density (light gray) sharply delineated by abrupt boundaries.

Grayscale density variations in the matrix were consistently observed across the S1 sample group, although differences in size and shape were noted between individual bread loaves. The coarse fraction, primarily composed of mineral components, was identified as the densest material in the samples, appearing light gray to white in color. Organic materials within the coarse fraction were identified in dark gray and, in some cases, exhibited densities close to air. Material identification was performed using X-ray attenuation, which is directly proportional to the density of the scanned material, enabling interpretation based on the grayscale map. Most voids in the S1 samples were flat and ranged in size from macro to micro. Channel and chamber voids were also identified, though some appeared ambiguously, partially filled with low-density material. In all S1 breads, voids containing plant fragments or those filled or partially filled with less dense material were observed. Notably, there was no sharp distinction between the bread's interior and crust. Instead, the matrix gradually transitioned near the edges, shifting from medium gray to dark gray tones over a narrow band (Figures 1A–L).

S2 breads (IB16 and IB42) exhibit the matrix with two distinct density zones separated by abrupt contacts. A third zone is present near the edge, where materials within the matrix are partially mixed, characterized by diffuse edges and a medium gray coloration. In this type of bread, voids and coarser organic material are not observable, and the contact between the dough and the crust is very distinct. The crust stands out from the bread dough. In some areas, the crust material overlaps, forming small folds, while it separates from the bread in other regions. It is not clear if the crust is composed entirely of the same material as the dough and detached by processing technique, or if it is a separate compound added to the bread. Still, it contains clear features of its physical separation from the dough matrix. Additionally, there is a difference in the grayscale density between the crust and the bread dough (Figures 2A–F).

TABLE 3 Description of 2 types of petrographic fabrics: type 1 for minerals fabric and type 2 for organic material fabric.

1 – Minerals fabric	Sample: IB01, IB08, IB09
Inclusions:	15%—25%; < 3 mm; equant to elongate; subrounded and rounded; single spaced; bimodal.
Predominant:	Biosilic, starch, around 0.02–0.05 mm, and organic fibers (around 0.01 thickness) (IB01 and IB08) Druses, around 0.02 mm (IB09)
Frequent:	Quartz, equant, sub-angular to rounded, max 0.2 mm, average 0.05 mm
Common:	Fragment Organic Material, elongate, max 3 mm
Few:	Charcoal, max 0.2 mm, average 0.05 mm (IB-01) max 0.5mm (IB09)
Rare:	Iron nodules, equant, max 1 mm; Feldspar microcline, max, 0.11 mm (IB09)
Matrix:	55%—75%; non-calcareous; heterogeneous; slightly optical activity. Color in PPL: brown-yellowish, brown-reddish, gray, limpidity: cloudy Color in XPL: dark brown, gray and brown-reddish, fabric-b undifferentiated (IB01 and IB08), striated (IB09). Presence of organic infillings, gray yellowish color, with limpidity dotted and fabric-b speckled
Voids:	10%—20%. Planes interlaced (meso and micro)
Aggregates:	Aggregates moderately to strong (IB01 and IB09) Weakly (IB08) separation, roughness mamillated, partial accommodation
Microstructure:	Granular microstructure
Observation:	Mineral Fabric is equivalent to S1 observed in Micro-CT and the massive characteristic in the sample hand.
2 – Organic material fabric	**Sample: IB16**
Inclusions:	49%; equant to elongate; rounded; closed spaced; unimodal.
Predominant	Starches, 0.02 mm; organic fibers, thickness 0.005 mm
Matrix:	50%; non-calcareous; heterogeneous; moderately optical activity. Color in PPL: yellowish and colorless, limpidity: cloudy Color in XPL: dark brown-yellowish and reddish, fabric-b speckled and undifferentiated
Voids:	1%. Planes, strong inclination, parallel (micro and meso).
Aggregates:	Aggregates with moderately strong separation, roughness mamillated, partial accommodation
Microstructure:	Massive and gum microstructure
Observation:	Organic Material Fabric is equivalent to S2 observed in Micro-CT and the spongy characteristic in hand samples.

3.2 Petrographic and mosaic analysis

In bread samples IB01, IB08, and IB09, the material exhibited a dense and compact structure with some reddish

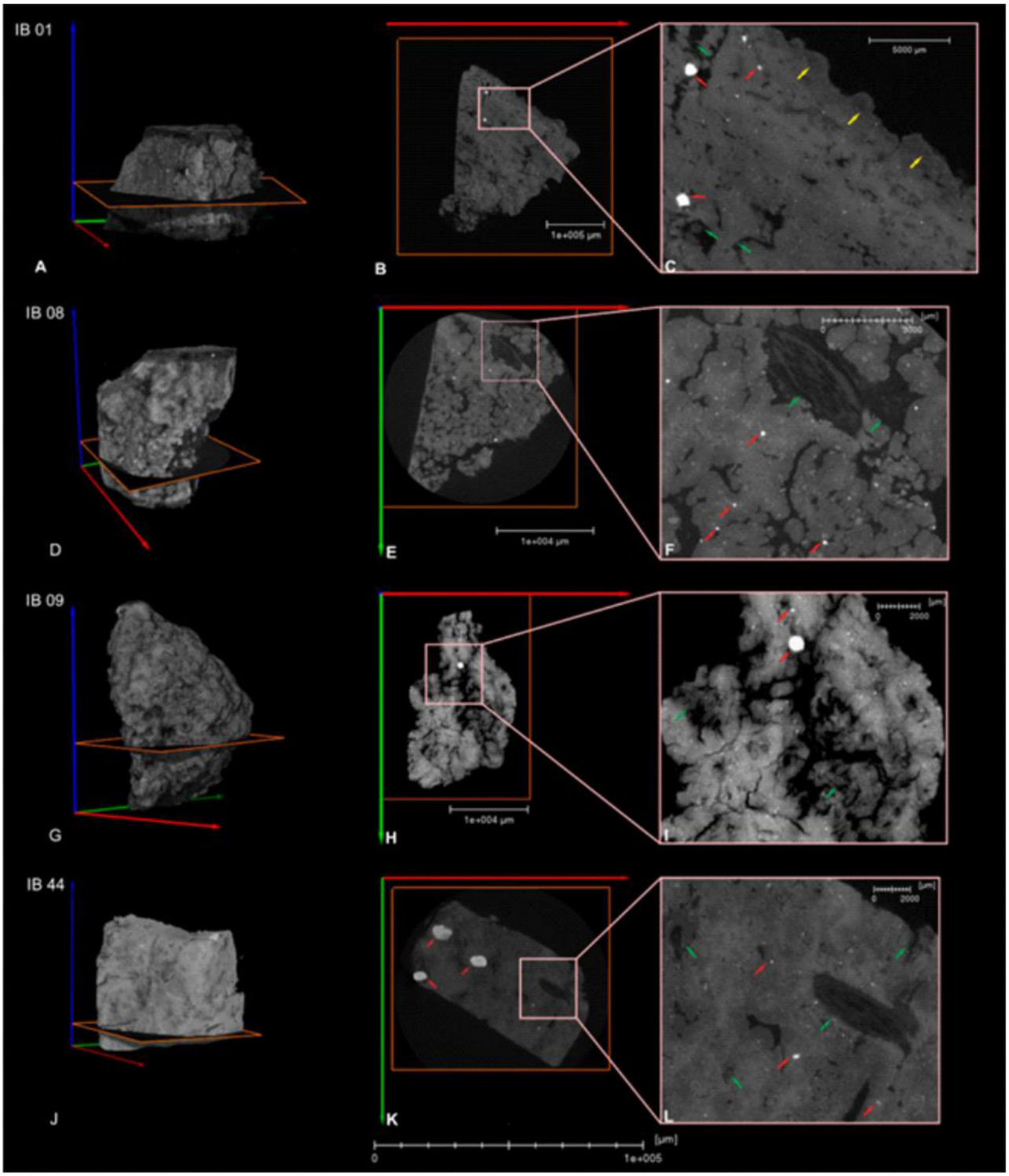

FIGURE 1
Micro-CT- Structure Type 01(S1) - **IB01, IB08, IB09,** and **IB44** – **(A, D, G, J)** Microtomographic fragments; **(B, E, H, K)** View section XY; **(C, F, I, L)** Details of fabric, with grayscale matrix, dark crust (yellow arrows), minerals (red arrows); and organic material (green arrows).

spots, small, blackened fragments, plant remains, and scattered whitish lines throughout the sample, all of which were visible to the naked eye. In IB09 it is possible to see sand grains. No void areas were observed. Stereoscopic analyses allowed for the creation of mosaics of the entire fragments and confirmed the presence of charcoal, clay nodules, and plant fragments on the surface of the sample. Additionally, the matrix displayed three distinct colors using the stereomicroscope: light brown, dark brown, and whitish. These characteristics are clearer in the mosaic of IB01, but the three

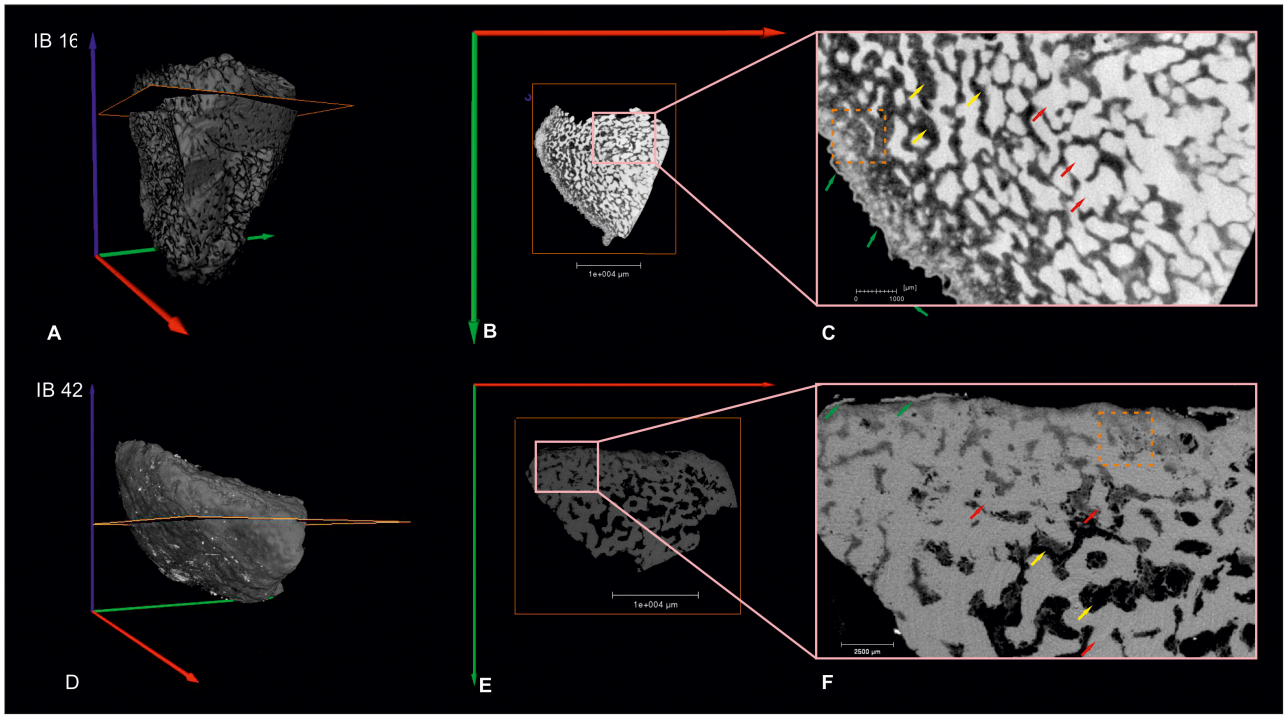

FIGURE 2
Structure type 02: IB16 and IB42: **(A, D)** Microtomographic fragments; **(B, E)** View section XY; **(C, F)** Detail View with different areas: Crust (green arrows); High dense area (red arrows); Light dense area (yellow arrows); Example of medium gray is the mixture area (red dotted square).

different colors and textures are present in all three samples (Figures 3A–J).

In IB16, a spongy mass with light brown and white coloration was identified with the naked eye. Stereoscopic analysis, in addition to constructing the mosaic of the fragment, revealed small, darkened spots, and reddish points. No void areas were identified (Figures 3K–M).

The differences in the mosaic images of IB01 and IB16 are discrete: the colors and textures of IB16 are noticeable to the naked eye, while the distinctions in the brown-toned areas of IB01 are less evident. Furthermore, IB01 contains fragments of clay nodules, plant macro-fragments, and wood charcoal, which are visible with the aid of a stereoscope.

The study of samples IB01, IB08, and IB09 confirmed the presence of organic and inorganic materials and an irregular microstructure. Notably, some void areas that appeared ambiguous in the micro-CT scans were determined to be filled with source organic material upon closer examination. In contrast, sample IB16 consisted of a mixture of starch and fibers, resulting in a compact biomass structure. Details of the different microstructure types are presented in Table 3, and specific descriptions of each sample are in the Supplementary material.

3.2.1 Fabric 1—mineral basis and granular microstructure

All samples with a mineral fabric exhibited similar characteristics, including quartz grains in the fine sand-silt fraction, iron oxide nodules, amorphous organic materials, plant fragments, and microcharcoals. Mineral fabric (F1) samples are classified as S1 in micro-CT analyses (Figures 4 IB01, IB08, IB09 A–F).

The matrix with a granular microstructure (Figure 4 IB08 A) shared common features: a yellowish-brown color in plane-polarized light (PPL) with a cloudy appearance, and a brown coloration in cross-polarized light (XPL). These matrices showed undeferential b-fabric in samples IB01 and IB08, and speckled b-fabric with low optical activity in sample IB09 (Figures 4 IB01 A, B; IB08 A, B; IB09 A, B). Additionally, coatings or infillings composed of organic materials or mixtures of organic and inorganic materials were observed in all samples (Figures 4 IB08 B, D).

Despite these similarities, notable differences were identified among the samples in this group. In bread IB01, the coatings contained starches and fibers, displaying a yellow to brown color in PPL, while the b-fabric was striated with moderate optical activity. The crust of this sample was also analyzed, showing a reddish-brown color in PPL and a dark brown color in XPL, along with identifiable microcharcoals. The coatings in bread IB08 were gray in PPL and mottled to undeferential in XPL, with phytoliths and partially degraded starches. In sample IB09, the coatings appeared in finer details, with a yellowish color in PPL, undeferential b-fabric in XPL, exposing only the druse with specific birefringence (Figures 4 IB09 A, B).

3.2.2 Fabric 2—organic material basis

Sample IB16 exhibited a compact microstructure, with planar voids occupying approximately 1% of the area

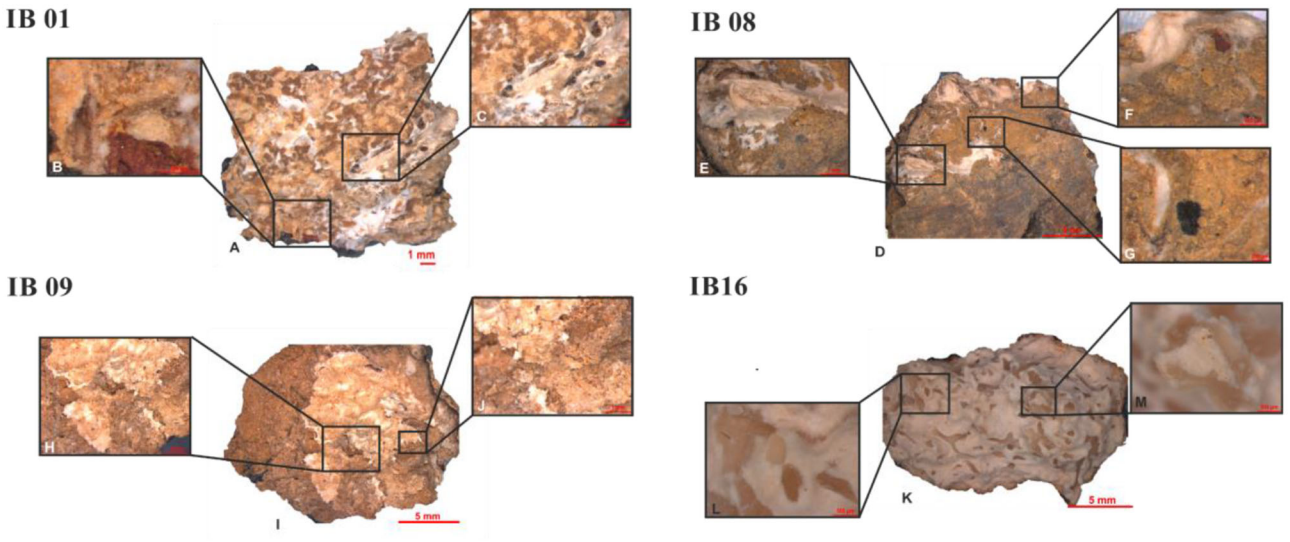

FIGURE 3
IB01: (A) Fragment mosaic image; **(B)** Iron nodule; **(C)** Plant residue; **IB08**: **(D)** Fragment mosaic image; **(E)** Fiber plant residue; **(F)** Iron nodule and white infillings; **(G)** Charcoal; **IB09**: **(H)** White Infillings; **(I)** Fragment mosaic image; **(J)** White and brown infillings; **IB16: (K)** Fragment mosaic image; **(L)** Spongy texture detail; **(M)** Fibers concentration with black and red spots. Images in oblique incident light.

(Figures 4 IB 16 C, D). The thin section showed two distinct regions under PPL: a yellowish area with a speckled b-fabric, ranging from gray to yellow and displaying high optical activity, and a second colorless area with an undifferentiated b-fabric (Figures 4 IB16 D–F). The crust of the sample was reddish under PPL and exhibited an undifferentiated b-fabric (Figures 4 IB16 A, B). This sample was classified as S2 in micro-CT analyses.

In the central region of the thin section, abrupt borders were observed between the colorless and yellowish materials. The colorless material was characterized primarily by the presence of microplanar voids (like cracks). Concentrations of starch and fibers were identified along the edges between the colorless and yellowish areas. Conversely, the yellowish area did not reveal identifiable starch grains or individual fibers (Figure 4 IB16 F).

Fluorescent light imaging showed that relatively well-preserved material was concentrated along the edges between the colorless and yellowish regions. Alterations to starches and fibers appeared to diminish closer to the crust, which presented a turbid appearance under PPL and high optical activity under cross-polarized light (XPL), indicating a process of gelatinization of the starches, typical of food processing techniques (Babot, 2003). This suggests that starch grains near the crust were better preserved than those in the bread's interior.

3.3 Experimental cassava (*Manihot esculenta*) flours

The experiments with different types of cassava flour aimed to understand how fibers behave during various flour-making processes. The initial step in making cassava flour involves grating the root, followed by washing and straining it to remove the juice, separate the dough, and decant the starch present in the water. In the bitter variety, washing is also part of the process to remove hydrocyanic acid, which is toxic to consumption. Different combinations of these elements lead to the creation of various products. A comprehensive discussion of the history, processing, and uses of cassava is available in França (2024).

This experiment specifically focuses on observing the behavior of cassava fibers after processing steps such as grating and separating the starch during flour production. Fibers are filamentous structures found in plants, particularly in roots and tubers. They can be classified as soluble, such as pectins and polysaccharides, or insoluble, like cellulose and lignin. It is important to note that Indigenous breads were not made exclusively or primarily with cassava; in some cases, cassava is absent while other lesser-known ingredients were used. After the European invasion, cassava gained greater prominence in the Amazon diet during the colonial period (dos Santos et al., 2021; França, 2024).

Yellow flour (YFS and YFT) is generally derived from bitter cassava, which contains hydrocyanic acid and must undergo several processing steps to become safe for consumption (Figures 5A, P). In contrast, white flour (WFB, WFS, and TFS) is made from sweet cassava, which is naturally free of toxins. Flour production requires grating, washing, and heating, except for tapioca flour (TFS), which also involves filtration, sedimentation, and decantation to extract starch from the dough. This sample showed a lower fiber content and a higher presence of starch and oxalates (Figures 5K–O).

Macroscopically, the YFT sample is notably rounded (Figure 5P), a feature attributed to the precise, repetitive movements performed by the flour maker during processing. This sample exhibited a higher number of aggregated fibers and starches, with fewer visible fiber clusters (Figures 5Q–T). In contrast, the YFS, WFS, and WFB flours, which have the most

10.3389/fearc.2025.1631639

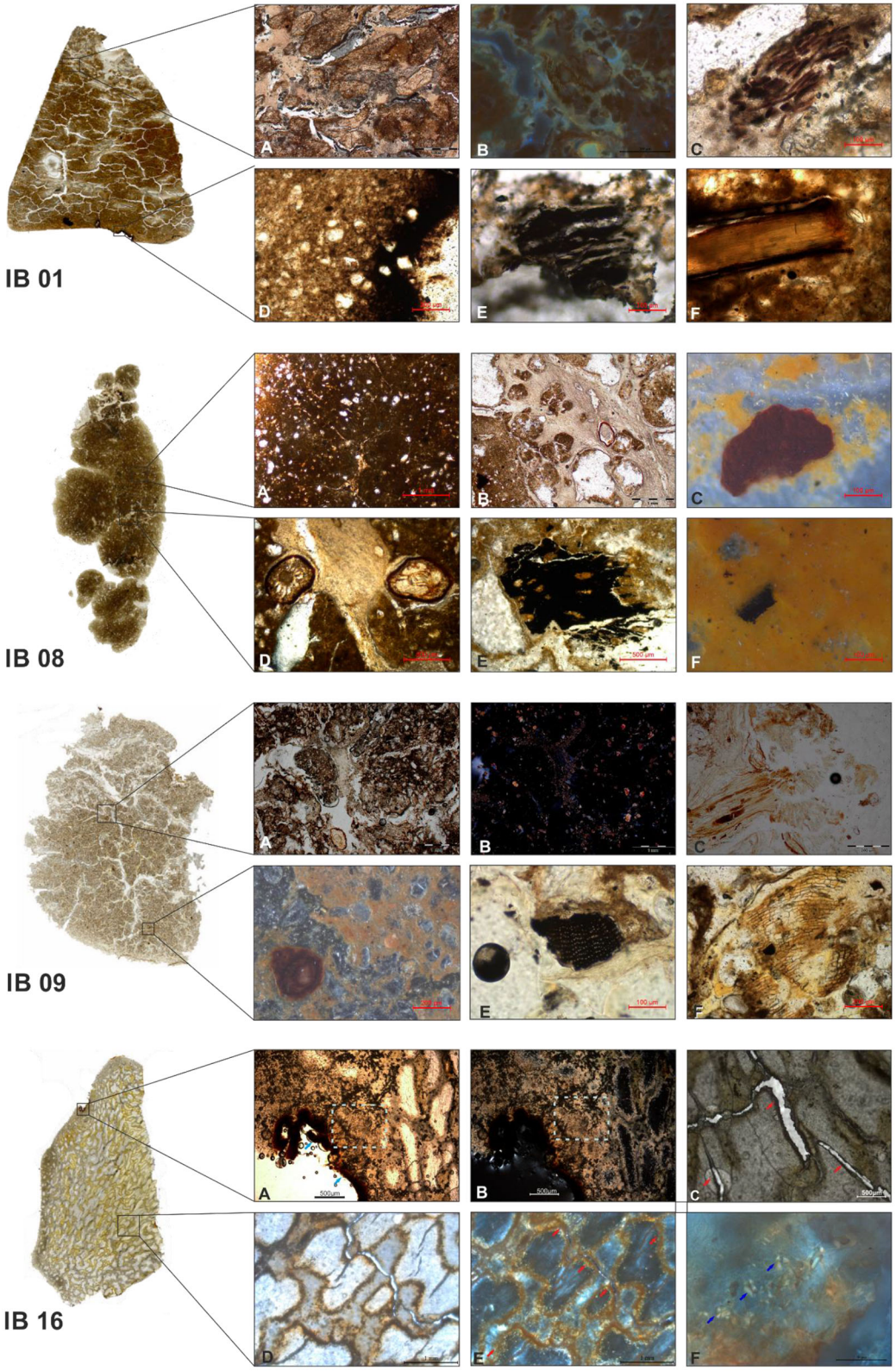

FIGURE 4
Petrographic photomicrographs of **IB01: (A)** Fabric with clay and organic coatings/infillings, 2,5x, PPL; **(B)** Organic coatings and infillings, 5x, FLS; **(C)** Amorphous organic material, 20x, PPL; **(D)** Crust and quartz grains, 10x, PPL; **(E)** Microcharcoal, 10x, PPL; **(F)** Plant residue. **IB08: (A)** Fabric, with clay and quartz grains 5x, PPL; **(B)** Organic infillings, 2,5x, PPL; **(C)** Iron nodule, 20x, OIL; **(D)** Organic infillings and fragment, 5x, PPL; **(E)** Charcoal fragments in micromass, 5x, PPL; **(F)** Microcharcoal, 20x, OIL. **IB09: (A)** Fabric with clay, organic fragment, and organic infillings, 2,5x, PPL; **(B)** Same, XPL: **(C)** Plant residue, 10x, PPL; **(D)** Iron nodule, 10x, OIL; **(E)** Charcoal, 20x, PPL; **(F)** Plant residue. **IB16: (A)** Fabric and Crust (blue arrow), an area with preserved starches (blue dashed square), 5x, PPL; **(B)** same, XPL; **(C)** Plannar voids, 10x, PPL; **(D)** Fabric and Voids, 2,5x, PPL; **(E)** Starches concentration area (red arrows), 2,5, XPL; **(F)** Starches, 50x, XPL.

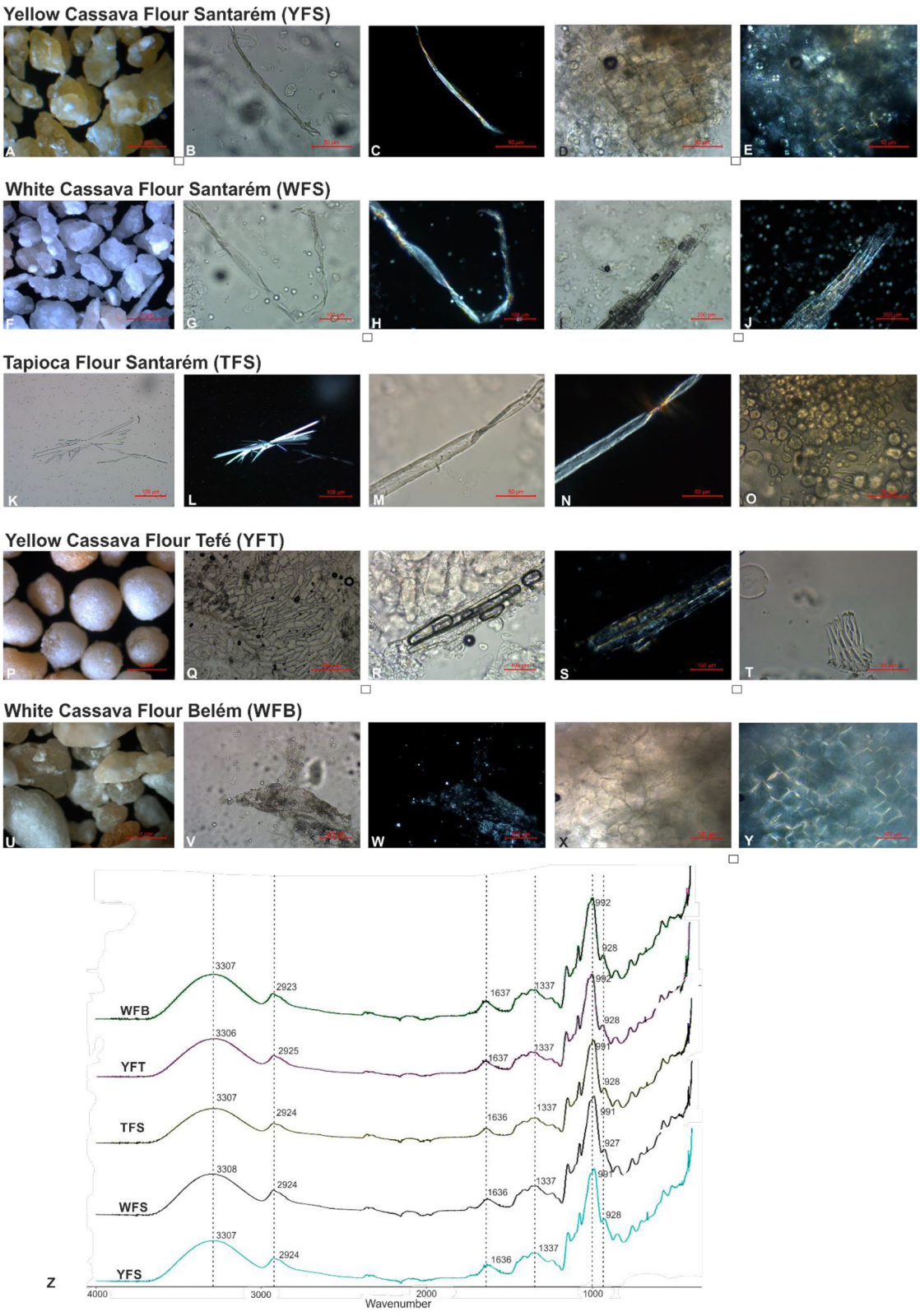

FIGURE 5
Cassava flour experiment: **YFS: (A)** Original sample, 2.5x, OIL; **(B)** Elongate fiber, 50x, PPL; **(C)** Same B, XPL; **(D)** Aggregates fibers, 50x, PPL; **(E)** Same D, XPL; **WFS: (F)** Original sample, 2.5x, OIL; **(G)** Elongate fiber, 20x, PPL; **(H)** Same G, XPL; **(I)** Aggregates elongate fibers, 10x, PPL; **(J)** Same I, XPL; **TFS: (K)** Oxalate, 20x, PPL: **(L)** Same K, XPL; **(M)** Elongate fibers, 50x, PPL; **(N)** Same M, XPL; **(O)** Starches, 50x, PPL; **YFT: (P)** Original sample, rounded shape, 2.5x, OIL; **(Q)** Preserved fibers, 5x, PPL; **(R)** Elongate fibers, 20x, PPL; **(S)** Same R, XPL; **(T)** Pioneer fiber, 50x, PPL; **(U)** WFB - U- Original samples, 2,5, OIL; **(V)** Aggregate fibers, 10x, PPL; **(X)** Altered starches -gelatinization process, 20x, PPL; **(Y)** Same X, XPL; **(Z)** FTIR spectra experiments sample.

angular shapes (Figures 5E, F, U), demonstrated more elongated and disaggregated fibers in their samples (Figures 5B–E, G–J, V–Y). Additionally, calcium oxalate crystals were found in the YFS sample but were absent in the WFS and WFB flours.

In addition to the fibers, starch also comprises an important component of cassava flour. Starch is a biopolymer composed of two polysaccharides: amylose and amylopectin, which serve as carbohydrate reserves in plants. Amylopectin is responsible for the crystalline structure of starch, while amylose contributes to its amorphous phase. Starches can be classified into Rapidly Digestible Starch, Slowly Digestible Starch and Resistant Starch, with their primary differences being in how their structures are altered. Heating starch in the presence of excess water results in the disruption of its crystalline structure, granule swelling, starch grain solubility, loss of birefringence, and changes in viscosity. The swelling factor of cassava starch is directly related to amylose and lipid content; higher levels of these components reduce water absorption capacity and consequently limit swelling. This process is known as gelatinization (Chisenga et al., 2019; Lacerda et al., 2009). Gelatinization of starch grains were observed in many archaeological contexts, including those previously described by Furquim (2024) for some archaeological Indigenous bread. Experimental studies have demonstrated it can derive from diverse cooking processes such as long periods of cooking, short periods of boiling (already after 5 min in some species), baking, popping and parching (Henry et al., 2008; Babot, 2003). These techniques cause different degrees of damage according to the plant species used and their time of processing and combination of procedures applied.

The retrogradation process occurs when gelatinized starch recrystallizes, often in mixtures with sufficient starch concentration, primarily driven by the reassociation of amylose. While this process is initially responsible for gel hardening, retrogradation is predominantly determined by the recrystallization of amylopectin over time (Chisenga et al., 2019; Versino and García, 2014).

In the FTIR spectra, no significant differences were observed in the peaks of the cassava flour samples. Compared to fresh cassava, the main expected changes include the narrowing of the O-H stretching band (3,300–3,500 cm^{-1}) due to reduced free water content and the reorganization of hydroxyl bonds. In the fingerprint region (1,200–900 cm^{-1}), changes in the crystallinity of starch lead to a transition toward a predominantly amorphous structure after gelatinization. The reduced or shifted peak around 1,020 cm^{-1} reflects the loss or reorganization of starch crystallinity, while the intense peaks near 930 cm^{-1} indicate an increase in amorphous structures (Versino and García, 2014; Qi et al., 2024). Although cassava is used as an example here, these spectral changes are characteristic of starch-rich organic materials and exhibit similar behavior across various samples, thus they do not show a "similar behavior," mainly in the relationship between crystalline and amorphous structures (Fornari Junior, 2017).

The cassava flour samples exhibited typical characteristics of organic material with starches, with bands associated with hydroxyl groups (O-H), C-H and C-O bonds, and the cyclic glucose structures. The bands at 3,307 cm^{-1} and 2,923 cm^{-1} reflect the presence of water and aliphatic bonds. The relationship between the band around 992 cm^{-1} and the bands at 1,077 cm^{-1} and 1,148 cm^{-1} reflects the vibrational modes associated with both the crystalline and amorphous forms of starch. Processing such as gelatinization, hydrolysis, or heating can alter the intensity and position of these peaks by affecting the starch's structure. The bands at 849 cm^{-1}, 759 cm^{-1}, 702 cm^{-1}, and 571 cm^{-1} are also indicative of the crystalline structure and the basic framework of starch (Figure 5Z). The relationship between the spectra and the images of the slides shows that there is good preservation of the cassava starches and fibers after the flour is made. The relationship between the spectra and the images of the slides shows that there is good preservation of the cassava starches and fibers after the flour is made.

This experiment aimed to compare plant fibers and starches of the cassava flour with materials found in the bread and to understand the behavior of starches through changes captured by FTIR spectra. The spectra were placed in the essential software library for comparison with the spectra of the Indigenous bread samples. Cassava has a low fiber content relative to starches (Navia and Villada, 2012), therefore, in the next stages of this research, it will be necessary to test other roots and fruits regarding their fiber and starch composition, such as yam (*Dioscorea* sp), mairá potato (*Casimirella* sp), and pupunha (*Bactris Gasipaes*).

3.4 FTIR

The spectra of the 16 breads were compared. The samples were divided into two groups (G1 and G2) based on the analysis of the most prominent peaks. G1 is characterized by a mixture, with the presence of unaltered or minimally fire-exposed clays in the central areas of the samples. The spectra of IB01, IB03, IB04, IB05, IB06, IB07, IB08, IB09, IB11, and IB44 indicate the presence of kaolinite in the clay fraction (Figure 6A). This is represented by absorption bands around 3,695, 3,645, 3,620, 1,030, 1,002, 911, and 529, corresponding to O-H stretching and structural vibrations (Berna et al., 2007; Weiner, 2010; Villagran et al., 2017). Quartz is also present, indicated by bands around 793 and 775. Samples IB01 and IB09 show a reduction in the intensity of kaolinite bands around 3,600 and the absence of the peak around 3,650, signaling thermal alteration of the clay (Berna et al., 2007; Weiner, 2010; Villagran et al., 2017).

G2 comprises materials formed primarily by starches. This is evidenced by absorption bands around 3,306, 2,925, and the sequence between 1,637 and 1,200. The presence of peaks around 1,024, and no peaks around 950, points to a significant change in crystalline structure of the starch to an amorphous one, probably by gelatinization (Versino and García, 2014; Qi et al., 2024). This group includes the central areas of breads IB10, IB12, IB13, IB14, IB16, and IB42 (Figure 6B). The compatibility of the samples with the spectra obtained from the flours indicated that samples IB10, IB12, IB13, IB16, and IB42 were compatible with WFB between 93% and 98%, while sample IB14 was 98% compatible with YFT (Figure 6C).

Samples from the crust of breads IB01, IB08, IB09, IB16, and IB42 were analyzed to compare with the central areas. The spectrum for IB01, IB08, and IB09 indicated the clay's thermal temperature alteration compared in the crust. Comparing the

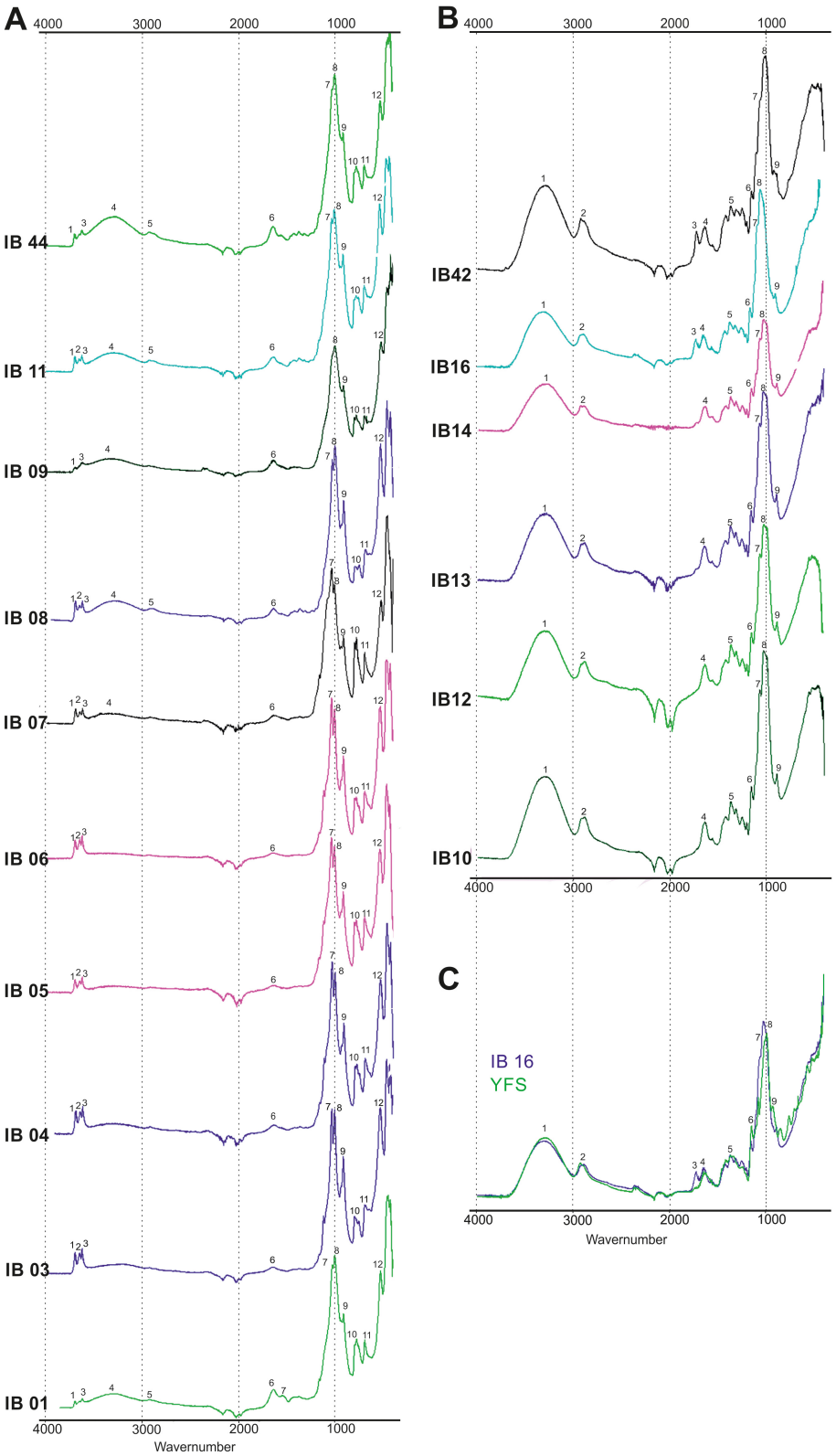

FIGURE 6
(A) Group 1 (Presence of kaolinite and organic matter) – 1, 2, and 3 represent the peaks around 3,695 cm^{-1}, 3,650 cm^{-1}, and 3,620 cm^{-1} (structural O-H); 4 represents the peak around 3,314 cm^{-1} (O-H hydroxyl); 5 corresponds to the peak around 2,920 cm^{-1} (C-H stretching), typical of organic material; 6 corresponds to the peak around 1,640 cm^{-1} (OH or adsorbed water); 7 corresponds to the peak around 1,534 cm^{-1}; 8: The peak between 1,412 cm^{-1} and 1,242 cm^{-1} represents the methyl, methylene, and C-O groups typical of organic materials; 9 and 10: The region where the Si-O stretching of kaolinite occurs, which may overlap and mask the C-O stretching from the organic material; 11: around 911 corresponds to the Al-OH stretching in kaolinite; 12: Peaks at 793 cm^{-1} and 775 cm^{-1} refer to kaolinite; 13: Peak at 691 cm^{-1} is characteristic of kaolinite; 14: Peak at 529 cm^{-1} is related to the Al-O-Si bonds in the kaolinite structure. **(B)** Group 2 (Starches organic material); **(C)** Comparing the IB16 with YFS.

spectrum, the center and crust are characterized by a reduction in the OH range between peaks at 3,695, 3,650, and 3,620, along with changes in the bands at 1,020 and 1,000. Additionally, prominent bands were observed around 3,300, 2,925, and between 1,630 and 1,200, suggesting starches organic material presence (Versino and García, 2014; Qi et al., 2024). For bread IB16 and IB42, the spectra showed the presence of kaolinite in the crust (Figures 7 IB16 and IB42 crust). The presence of peaks 3,686 and 3,624 and the loss of the peak near 3,650 is typical of the progressive loss of hydroxyls during the heating of kaolinite and the transformation to meta kaolinite. However, the preservation of the nearby doublets 794 and 778 (Si-O-AL), the 692, 517 shows that kaolinite structure is still preserved. This clay may have come from the soil during burial, however from the Micro-CT observations and petrography, the clay may have been used to intentionally coat the bread to help create the crust.

The infillings observed in the slides of fabric 1 were identified as amorphous materials with a white to yellowish coloration in hand samples. It was possible to extract these materials from breads IB01, IB08, and IB09. In the spectra of IB09 and IB08, peaks corresponding to starches, organic material, and clay were detected (Figures 7 IB08 and IB09 white infillings). In sample IB01 however, the spectrum revealed only organic material (Figure 7 IB01 white infillings). The compatibility of the samples with the spectra obtained from the flours indicated infillings samples IB08, IB09 were compatible with WFB between 98% and 95%, while sample IB01 was 97% compatible with YFT. For IB44, a red, rounded particle embedded in the dough was analyzed, and its spectrum was consistent with kaolinite.

4 Discussion

All the methods applied in this study indicate the presence of at least two groups of breads, distinguished by their structure, matrix, and composition. Type 1 breads are described as having massive characteristics observed in the Micro-CT as Structure 1, identified in petrographic analysis as Fabric 1, and belonging to Group 1 in the FTIR analyses, which revealed the presence of starch and plant parts, along with clay and quartz grains in their composition. These samples are primarily represented by IB01, IB08, IB09, and IB44, which underwent FTIR and at least one imaging analysis. Additionally, samples IB03, IB04, IB05, IB6, IB07, and IB11 displayed spectra compatible with Group 1 and likely shared the other observed characteristics. The systematization is presented in Table 4.

Type 2 breads are characterized as spongy and correspond to Structure 2 in the Micro-CT, Fabric 2 in petrography, and Group 2 in FTIR analyses. The most representative samples of this group are IB16 and IB42, which were analyzed with image methods, but IB10, IB12, IB13, and IB14 also exhibited spectra consistent with Group 2 and are likely part of this group. This type is marked by the presence of fibers and starches around 10 μm and lacks coarse organic fragments, quartz grains, and clay.

One of the main objectives of the image analysis of this material was to examine the formation of structures resulting from fermentation. Studies on fermentation processes suggest that microporous and closed voids are formed by the trapping of gases produced during fermentation. Additionally, during baking, the expansion of air can form a network of open voids (Arranz-Otaegui et al., 2018). However, no such voids were identified in the micro-CT or petrographic analysis of the bread samples. Furquim (2024) reported the presence of starches with damaged features indicative of fermentation. Three possible explanations for this discrepancy are: the dough may have undergone a low degree of fermentation; fermentation may have occurred with the ingredients separated or the high fiber content in the samples may have hindered bubble formation. Further experimental research will be necessary to explore these possibilities.

4.1 Production and process

4.1.1 Indigenous bread—type 01: massive structure with organic material, quartz grains, and clay

In micro-CT analysis, the low attenuation coefficient of organic material can be like that of air, leading to the potential misinterpretation of areas with organic residues as voids (Villagran et al., 2019). However, when examining thin sections of samples of the fabric 1, it was possible to identify that some of the voids observed in samples S1 the micro-CT scans were filled with fine organic materials in the form of coatings and infillings, exhibiting a fabric-b ranging from mottled to undifferentiated (Figures 8A–C, N–R, X–AB). Upon re-examining the bread samples, this material was identified as the white mass filling the spaces between brownish aggregates within bread samples IB01, IB08, and IB09 (see Figure 3).

This deposition between aggregates altered the configuration of voids in the samples. The production of these breads appears to have occurred in distinct stages: (1) Initial Dough Preparation - The dough was prepared with fresh ingredients processed into a flour, creating a moist texture, which allowed for the formation of larger voids as air was trapped during mixing and kneading; (2) Moistening of the dough - The dough was subsequently moistened, which altered the areas containing organic materials and filled the voids, creating coatings and infillings. Between stages 1 and 2, a period of dough rest is necessary. This is because the dough contains primary voids probably formed during kneading, and secondary planar voids, probably resulting from the drying of the dough. Afterwards, both types of voids are almost filled. Another possibility is that the dough was constantly moistened after receiving its final shape, as the infilling and coatings do not show signs of post-formation alteration. This process likely increased the amount of organic material and caused the density changes observed in microtomography as mottled areas, typically around voids, with a gradual grayscale variation from light to dark. A similar process is reported by Gumilla (1745) in his description of bread-making by the Otomacos in Venezuela. In their preparation, the mass is intensively washed and sieved.

Plant residues appear in a wide variety of sizes, shapes, and distributions. In the micro-CT analysis, all samples with this fabric 1 exhibited macro-sized plant fragments. Petrographic analysis revealed differences in the composition of each bread. For example, IB01 is rich in fibers and starches (Figures 8D–H, J–M) and appears

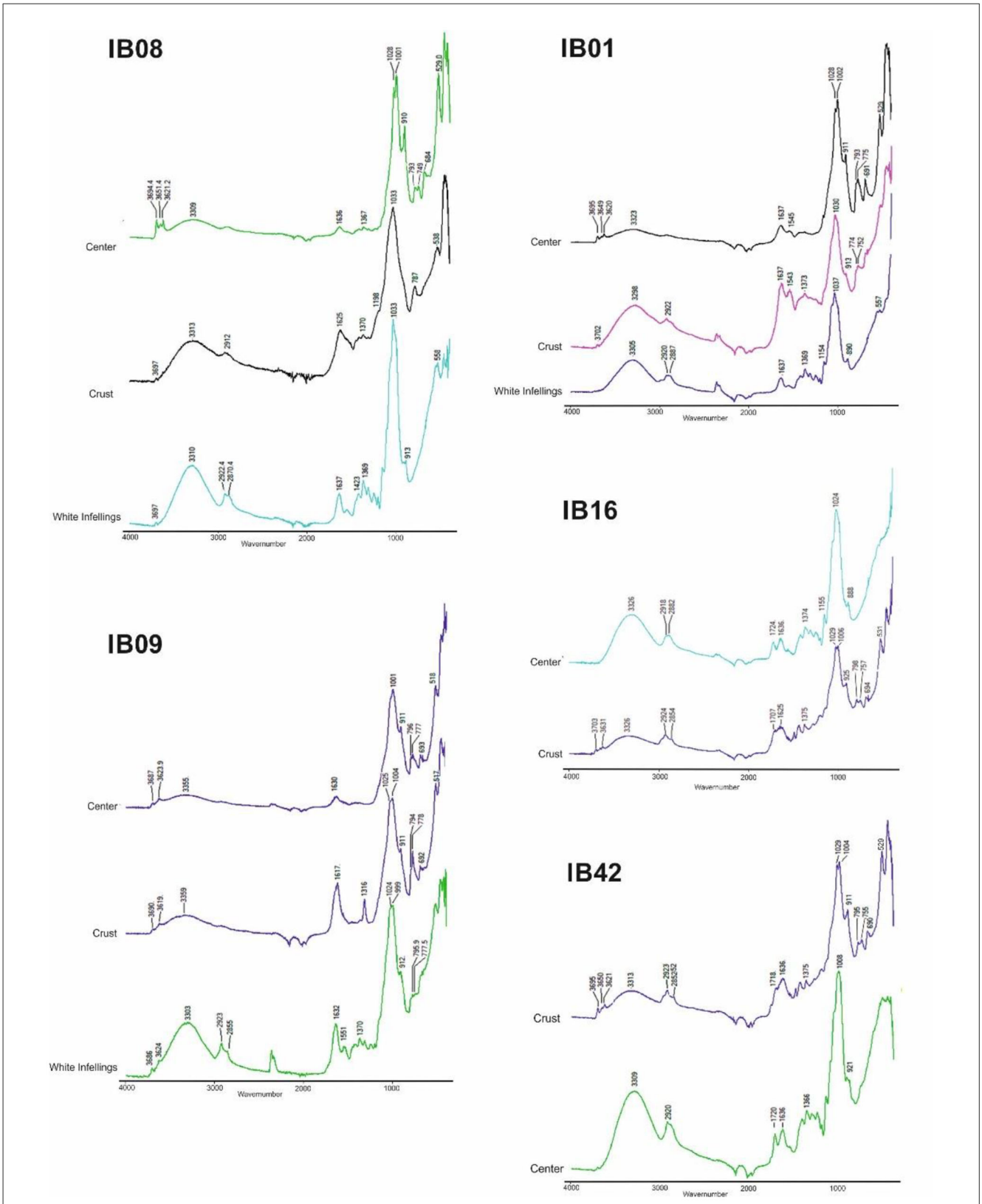

FIGURE 7
IB09, IB08, and IB42 – The spectra from the center and the crust show peaks around 3,690 and 3,620 cm^{-1}, associated with the presence of clays, especially in the center of the bread. In IB01 and IB42, however, these clay peaks appear modified by the effect of fire in the crust, particularly in the bands near 3,690 and 3,620 cm^{-1}.

TABLE 4 Summary results of analysis.

Sample's code	Hand sample	Micro-CT	Petrography	FTIR
IB01	Massive	Structure 1	Fabric 1	Group 1
IB03	Massive			Group 1
IB04	Unidentified			Group 1
IB05	Unidentified			Group 1
IB06	Massive			Group 1
IB07	Massive			Group 1
IB08	Massive	Structure 1	Fabric 1	Group 1
IB09	Massive	Structure 1	Fabric 1	Group 1
IB10	Unidentified			Group 1
IB11	Unidentified			Group 2
IB12	Spongy			Group 1
IB13	Spongy			Group 2
IB14	Spongy			Group 2
IB16	Spongy	Structure 2	Fabric 2	Group 2
IB42	Spongy	Structure 2		Group 2
IB44	Massive	Structure 1		Group 1

to have a fungal surface with the presence of hyphae (Figures 8I, J), but specific studies are needed for confirmation, IB08 contains biosilica and starch without birefringence (Figures 8S–W), and IB09 demonstrates high concentrations of druses and fibers (Figures 8AC–AG). These differences are probably directly related to the different ingredients used in each recipe and the plants' characteristics, starch structure. However, it was not possible to identify the plant species utilized, requiring additional methods such as the macro residue, phytolith, or starches and lipids analyses as performed by dos Santos et al. (2021) and Furquim (2024).

Fibers were present in all petrographic samples. The structure of these fibers images are elongated filaments 10–50 mm thick (Figures 8I, L, AG), resembling the overall structure of cassava fibers (Figueiredo et al., 2015), and it is likely that its similarity to fungal hyphae may have contributed to the long-time classification of these breads as fungi. Fungal hyphae differ from plant fibers under polarized light. While plant fibers exhibit high birefringence due to the alignment of cellulose molecules, fungal hyphae, with rare exceptions, exhibit little to no birefringence (Stoops, 2021; Fitzpatrick, 1984). Recent studies analyzing different samples of Indigenous bread, including the present one, refute the hypothesis that these loaves are fungal (dos Santos et al., 2021). Considering the use of 11 species of fungi in the Yanomami Indigenous land and other records in the Amazon (Sanuma et al., 2018; Putzke et al., 2021; Pereira et al., 2018), along with fungus-facilitated fermentation and the biodiversity of the Amazon, it is plausible that wild fungi could have been part of the ingredient list and even played an important role in the fermentation process. A new mycology study looking at fungi as a potential ingredient or process result, rather than bread as a large mycelium, will bring important contributions to the understanding of the process of ancient Indigenous bread production.

Nevertheless, it is also highly likely that many of the fibers observed in the thin sections are fragments of fibrous plants due to the presence of birefringence when polarized (Figures 8L, AG). Some of these plants, such as cassava and sweet potato, have already been confirmed as sources of starches in certain bread samples (Furquim, 2024). Cassava contains diagnostic starches, many of which are embedded within fibrous structures. To extract these starches effectively, it is necessary to break down the fibers, often achieved by grating the cassava (Feniman, 2004).

Petrographic analysis showed a well-defined crust with dark coloration and a fabric-b undifferentiated (Figures 9A–C, G–I), but the micro-CT revealed a diffuse area indicating a slight density change. Spectrometry analysis provided further insight into these variations, suggesting they might be related to low-temperature heating. Preserved organic matter supports this hypothesis, which would have been lost at higher temperatures.

For bread samples IB09 and IB01, evidence suggests they were subjected to heat. However, no significant differences were observed in the spectra of the bread's center compared to its crust. This may indicate effective process control, ensure uniform heating and suggest that the bread was not in direct contact with the heat source and was in controlled exposure to heat, such as smoking.

The formation of the crust differs among the samples. There is evidence of clay heating in IB01, IB08, and IB09, in addition to a greater presence of organic material (Figure 9J). One hypothesis is the application of an organic substance on the bread's surface before burial, which could have contributed to the formation of a crust and helped preserve the bread during burial.

Image analyses of samples IB01, IB08, and IB09 revealed randomly dispersed quartz particles and clay nodules within the bread (Figures 9D–F, K, L, M–O). Initial hypotheses suggested that the quartz grains could have been introduced into the dough during grinding the plant components with a stone mortar and pestle, during baking in a ground oven, or could be related to the method of preparation.

However, considering the image analyses and the spectrometry results—12bread loaves out of 15 analyzed have clay in their fabric, and all samples in FTIR analysis from Group 01 exhibited both clay and quartz in the bread dough—the recurrence of their presence may indicate a widespread pattern included in the bread technology. This suggests that clay may have been intentionally added to the dough as an ingredient—not necessarily for gaining flavor, but for gaining texture or other nutritional purposes.

4.1.2 Indigenous bread—type 02: spongy structure with organic material

For samples IB16 and IB42, no voids were identified in the micro-CT analysis. In the petrographic analysis of sample IB16, planar voids were present in about 1% of the area, with meso- and micro-sized voids. The micro voids were observed in large quantities, appearing parallel and interlaced in the colorless areas formed by starch gelatinization (Figures 10H–J). The final formation of planar voids is associated with the drying process of the material, which could have occurred either through rapid drying due to heat exposure or during exhumation when the dough lost water.

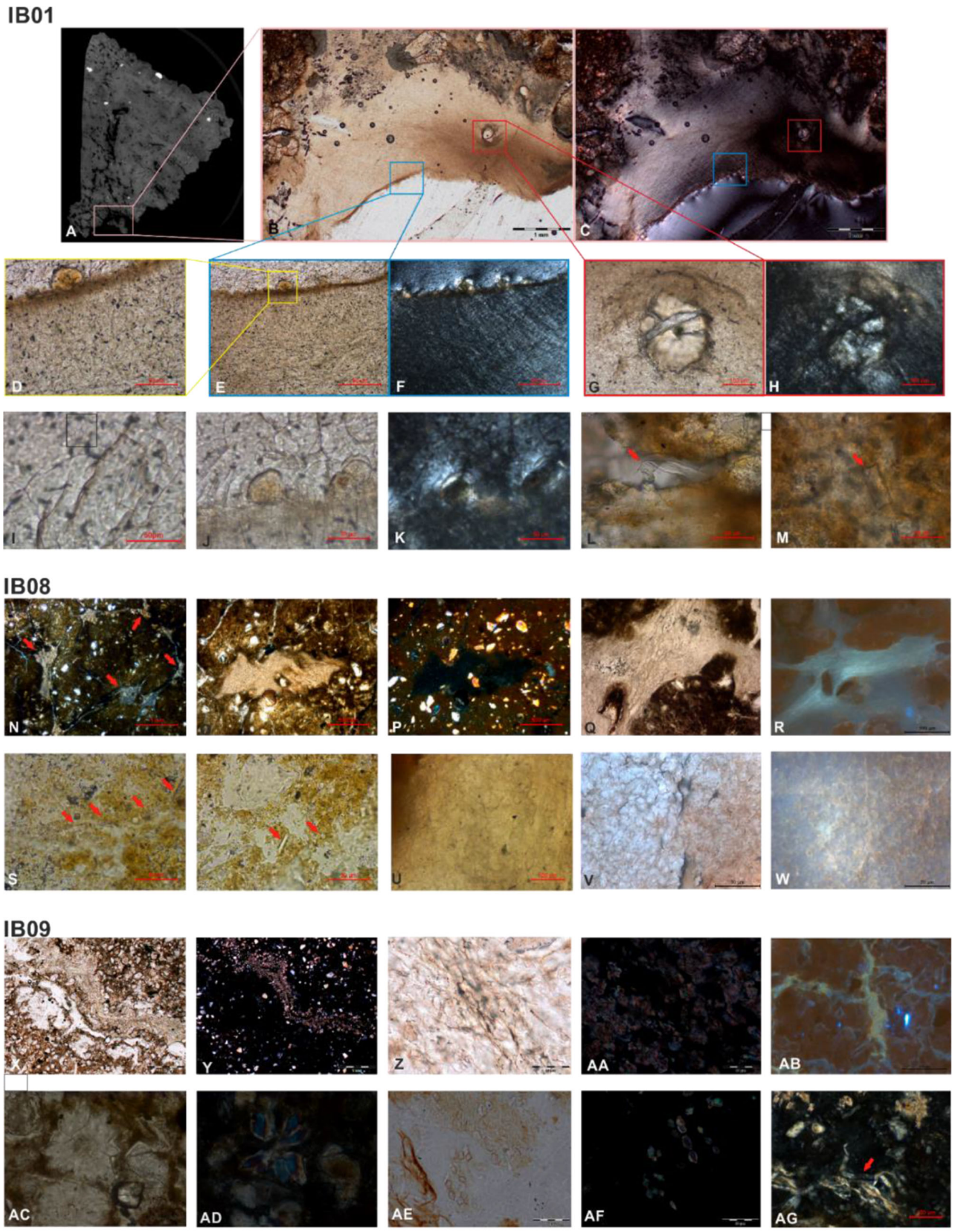

FIGURE 8
IB01: (A) Micro-CT image appoint the Infillings in the sample. **(B)** Infillings, 2.5x, PPL; **(C)** Same B, XPL; **(D)** Details of the edge of infillings with starches deposited, 50x, PPL; **(E)** Details of the edge of infillings with starches deposited, 50x, PPL; **(F)** The same E, 20x; **(E)** the same F, XPL; **(G)** Grain
(Continued)

FIGURE 8 (Continued)
was deposited during the filling formation, so it is possible to observe the deformation of the material, 50x, PPL; **(H)** Same G, XPL; **(I)** Probable fungal hyphae. 50x, PPL; **(J)** Starch grain on the surface of the bread is surrounded by probable fungal hyphae., 50x, PPL; K- same J, XPL; **(L)** Fiber mixture with clay, 50x, PPL; **(M)** Biosilic, 50x, PPL; **IB08: (N)** fabric with aggregates and infillings in the voids (red arrows), 2,5x, PPL; **(O)** Infilling with a quartz grain inside, 5x, PPL: **(P)** Same O, XPL; **(Q)** Details of the infillings, 10x, PPL; **(R)** Details of infillings with aggregates inside. 5x, FLS; **(S, T)** Biosilica, 50x, PPL; **(U)** Infillings details with altered starches, 20x, PPL; **(V)** same U, 50x; **(W)** Same V, FLS; **IB09: (X)** Infillings with druses, 2,5x, PPL; **(Y)** same X, XPL; **(Z)** Details infillings with druses, 50x, PPL; **(AA)** Same Z, XPL; **(AB)** Fabric with highlighting infillings, 50z, FLS; **(AC)** Druses mixed into the clay, 50x, PPL; **(AD)** Same AC, PPL; **(AE)** Diamond-shaped druses, 50x, PPL; **(AF)** Same AE in XPL; **(AG)** Druses and fibers (red arrow), 20x, PPL.

The organic material in samples IB16, which are associated with microfabric 2 in petrographic analyses, was well-processed, with no visible macro residues and the presence of phytoliths, starch and fibers (Figures 10K–M). The ingredients likely underwent intense processing, using techniques that involved high moisture content and heat, resulting in partial damage to the starches. The starch damage resulted in gelatinization and loss of birefringence. In areas where starches are well-preserved, there is strong fiber intertwining (Figure 10M). This process transformed the starch into a gelatinous form, observed in petrography as a colorless area and in micro-CT as a dense region. The process of starch gelatinization and its conversion into a colorless film is well-documented in the food industry (Chisenga et al., 2019; Diabor et al., 2019), biotechnology research (Teodoro et al., 2015; Paes et al., 2008; Abdullah et al., 2018), and experimental archaeology of plants and cuisine (Henry et al., 2008; Babot et al., 2014).

In the microtomography of samples IB16 and IB42, the separation into distinct areas provides insights into the dough's malleability during the production process and the drying. The parallel orientation of colorless and yellowish areas was observed in regions where pressure points occurred during bread production and dough folding (Figures 10A, B). Additionally, the central region of the bread likely remained moist for a longer time, leading to a greater degree of gelatinization. This resulted in larger colorless areas with abrupt edges. In contrast, water dried more quickly near the edges, creating smaller colorless areas where starches did not have sufficient time to undergo alteration, forming a diffuse part in the dough. This rapid drying of the area near the border is likely a consequence of heating.

Microtomography also reveals well-defined crust areas in samples IB16 and IB42, with some regions appearing to detach from the bread (Figures 10A, B). Petrographic images of sample IB16 show a well-defined area, red in PPL and undifferentiated in XPL. In the area near the crust, fibers and starches are visible and well-preserved under parallel-polarized light (PPL). However, under cross-polarized light (XPL), the area does not exhibit birefringence, likely due to heat exposure (Figures 9F, G). Another important detail is the folded region of the bread. In the micro-CT image, the crust appears well-preserved between the folded sections, indicating that the bread was still flexible when the crust formed (Figure 9A). Spectral analyses of both samples indicate traces of clay in the crust. This clay may have originated from the soil where the samples were buried. However, its uniform impregnation on all sides and the crust coming off suggests it might have been intentionally applied as a protective layer, helping to form a crust around the dough before heating (Figures 10A–G).

4.2 Indigenous bread and ancient food technology

The presence of identified features in the bread recovered from different parts of the Amazon basin attest to the diversity of ingredients and biotechnologies related to its production and storage. It is a widespread technology of dough preparation and food storage, and its importance has only recently been recognized (dos Santos et al., 2021; Furquim, 2024). Due to the absence of contemporary examples of the burial of bread in the Amazon, it is necessary to evaluate these remains following the wide ray of foodways and practices related to nutrition and medicine developed and maintained by contemporary Indigenous people. This involves experimental archaeology and long-term Indigenous history perspectives, by connecting ancient to modern food technologies. Many of the features identified in this research are closely related to practices acknowledged in different parts of the basin (dos Santos et al., 2021; Furquim, 2024; França, 2024).

The presence of quartz and iron nodules may be suggestive of the many aspects of food preparation, processing, and storage acknowledged by Indigenous people. The contact of food with minerals can be hypothetically traced back to the use of stone tools to process plant parts—such as grinding stones or mortars—or to the use of earthovens. Ethnographic records indicate that *paparuto*, a traditional and ceremonial cassava flat bread of the Krahô ethnic group, is prepared on leaves on the ground and baked in the *moquém* (a hearth constructed by digging a shallow holeand adding firewood or rocks for cooking) covered with earth, which may have resulted in the accidental incorporation of these grains (Krahô et al., 2005). Many archaeological sites in the Amazon basin demonstrate evidence for the use of stone mortars to grind seeds and roots, such as the Teotônio site (Paulo, 2019), and many ethnographic descriptions attest to the use of grinding stones, such as the Baikarí as told by den Steinen (1940).

The presence of microcharcoals and thermal alteration in the crust, where both organic and inorganic matter presents signals of heating, is suggestive of the use heating. We hypothesize that it may have been smoked, considering the crust formation and the differences observed through FTIR in the internal and external areas of the bread. The hypothesis of food smoking practice, made by adding the meal or separate ingredients to a *girau,* a hardwood or palm wood grid located above the hearth at variable distances (according to the results wanted) or along the house roof—that produce light and continuous heating during long periods of days or even years. Smoking is a food preparation and conservation technique common to many Indigenous groups in the Amazon. Some examples include peppers (*Capsicum* sp.) in the Upper Negro

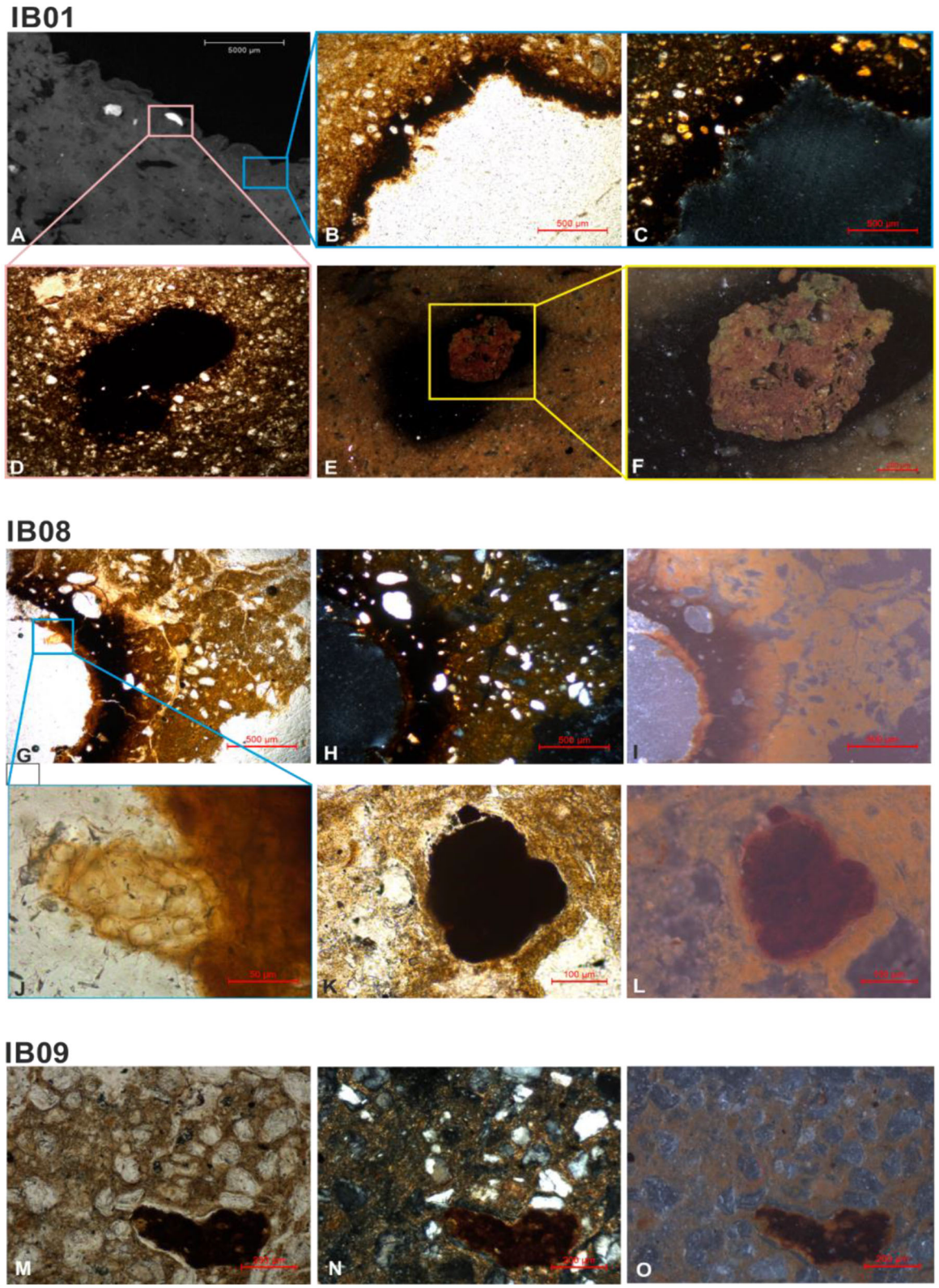

FIGURE 9
IB01: (A) Micro-CT image highlighting the clay nodule and crust of the bread; **(B)** Crust and some quartzes grains, 5x, PPL; **(C)** Same B, XPL; **(D)** Clay nodule, 5x, PPL; **(E)** Same, OIL; **(F)** Detail of clay nodule showing different colors, and quartz grains, 10x, PPL. **IB08: (G)** Crust, some quartz grains and an organic material put after the crust formation, 5x, PPL; **(H)** Same G, XPL; **(I)** Same G, OIL; **(J)** Detail of organic material in the crust, this rounded is altered starches, 50x, PPL; **(K)** Clay nodule, 20x, PPL; **(L)** Same K, OIL. **IB09: (M)** Fabric with a clay nodule, 10x, PPL; **(N)** Same M, fabric-b striated, with a granostriated, XPL; **(O)** Same M, OIL.

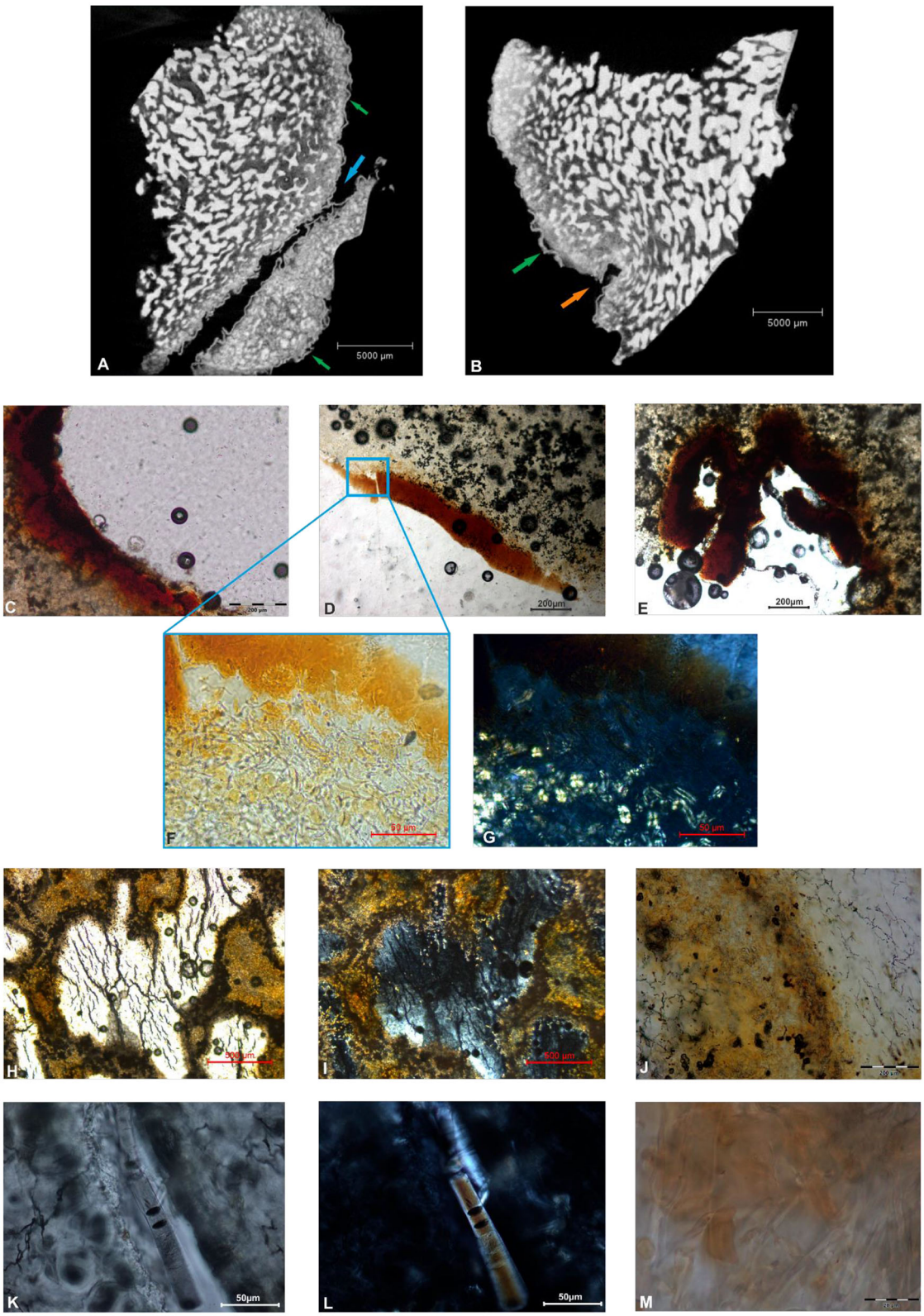

FIGURE 10
IB16: (A, B) Micro-CT image: Crust (green arrows), pressure point organizing the spongy structural parallel around the point (orange arrow), folding the bread dough (blue arrow); **(C–E)** Different parts of crust, 10x, PPL; **(F)** Detail in area near the crust with the preserved starches and fibers, 50x, PPL; **(G)** Same F, It is possible to see part of the material near the crust without birefringence, probably material altered by heat; **(H)** Crack area, 5x, PPL; **(I)** Same H, XPL; **(J)** Details of the crack area, 10x, PPL; **(K)** Biosilica, 40x, PPL; **(L)** Same K, XPL; **(M)** Starches and fibers, 100x, PPL.

River (França, 2024), the *payá beiju* flat bread of the Kaxuyana et al. (2024), the Enawene-Nawe loaves of cassava (Mendes dos Santos, personal observation), as well as the widespread use of the *moquén* (long and light smoke) to prepare meat. It is also worth mentioning that there are some descriptions of the application of tree resins to the outer surface of foods to avoid spoilage. The Nukini people, part of the Pano linguistic family, report old recipes of bread made by their ancestors from corn and macerated cassava, coated with latex from the rubber tree (*Hevea brasiliensis*) (dos Santos et al., 2021). However, when comparing the FTIR spectra of the bread crusts from IB08 and IB09 with FTIR data from the literature on rubber tree latex, no spectral match was observed, neither at room temperature nor when heated to 100 °C (Ibrahim et al., 2014; Rolere et al., 2015). Another possibility is the use of natural resins or even the juice of starch-rich plants, as reported by Gumilla (1745).

The consumption of clay is a practice documented in historical and ethnographic descriptions of the foodways and medicines in the Amazon (Gumilla, 1745; Spix e Martius, 2017) and played multiple roles in the culinary and cultural practices of various Indigenous groups in South America and elsewhere. Father Gumilla (1745) and Von Humboldt and Bonpland (1852) both describe clay consumption among the Otomaco ethnic group in the Orinoco River. It is interesting to note that these authors disagreed on the role of the intentionality and function of inorganic materials. While Gumilla describes inorganic matter as an ingredient for the production of nutritious bread, Humboldt focused on the physiological aspects of consuming clay.

According to Gumilla, bread was made with corn, cassava, and various other local fruits they cultivated, after macerating it and burying it in holes along the banks of the river. After a few days, the mixture was unearthed and mixed with local clay, forming a dense dough containing starches and clay. It then underwent a process of kneading and sieving to remove part of the water. This dough was then combined with turtle or alligator fat, kneaded, and shaped into balls, dried in the sun, and baked. Gumilla observed that the Otomacos carefully selected the clay and were skilled at locating it along the river. In contrast, Humboldt described eating clay as a physiological phenomenon related to food scarcity. He observes piles of *poya*, a specific soft clay, greasy to touch, and either gray or yellowish, that were collected from alluvial areas or smoother, oilier layers that seemed to contain decomposing organic material. The *poya* was baked, giving it a reddish color, and consumed. Moreover, for the Negro River, Spix e Martius (2017) described the consumption of cassava, pirarucu (*Arapaima gigas*), and *tabatinga* a type of clay found in specific banks of the river, that could be gray, yellowish, or greenish. They noted that this practice extended to other parts of the Amazon.

In recent times, the Villas Boas brothers (Simões, 1981) have conducted a large enterprise of contacting Indigenous people for a national policy of integration and reported from the Juruna informants that the Txukahamãi living in the neighboring Xingu River area had the habit of eating clay. The consumption of termite mound soil was also observed on two occasions. The first occurred when remains of termite mounds, burned in a bonfire, were consumed. The second took place during a trail walk, where the Txukahamãi removed and savored pieces of the termite mound. The Baikari people of the Teles Pires River recounted that their ancestors, lacking knowledge of corn and cassava, resorted to eating clay. They also created small clay dolls, which they gave to children to lick (den Steinen, 1940). Finally, the Paliukur people regularly consumed a special clay called *paraukama*, rich in iron and manganese oxides (Fernandes, 1950).

It is important to note that contemporary and ancient peoples around the world consume clay beyond physiological needs, reflecting cultural practices and religious beliefs. From *Homo habilis* occupations (Clark, 2001), descriptions made by Hippocrates in the 4th century (Adams, 1886), and through the 19th century Nordic region, the consumption of clay is undoubtedly widespread. Some of those practices were related to bread making in some villages in Sardinia, for example, bread (*pa'n ispeli*) was made by mixing acorn flour with iron-enriched clay soil (*trokko*) to neutralize tannic acid (Laufer, 1930). The incorporation of clay into the bread dough we are analyzing is a plausible hypothesis, especially after comparing the results of this study with the use of clay in Indigenous culinary practices. The use of clay in food, as documented in the Otomacos and other groups, not only meets nutritional needs but reflects a deeper cultural and ecological connection to the environment. This broader understanding suggests that intentionally incorporating clay in food preparation may be more common and meaningful than initially thought.

5 Conclusions

Indigenous Breads are records of a rich tradition of ancestral food technology that has crossed generations throughout the Amazon, and only recently has scientific research begun to delve deeper into this knowledge, which has always been present in the oral traditions of different indigenous groups and riverside communities. Through geoarchaeological and micro archaeological approaches, integrating different imaging methods, FTIR, and experimental studies, it was possible to confirm the presence of organic and inorganic matter and classify the bread samples into at least two types: (1) one with a massive appearance, incorporating clays and mineral grains, and (2) one with a spongy texture, prepared from roots with a high starch content. Furthermore, the production of these breads highlights the complexity of the preparation process, from the use of different ingredients to the various stages of preparation, such as kneading, starch preparation, gelatinization processes, dough wrapping, smoking and ultimately culminating in burial. This study demonstrated that Amazonian food conservation and storage technology was sophisticated, with controlled methods of processing and heating, as well as a deep and careful interaction with the environment and available resources. The use of clay yet another food and conservation ingredient only confirms the diversity of foodways among the different Amazonian ethnic groups.

The production of food surpluses and the storage of food have been a key concern since classic studies relating foodways and social organization in the Amazon basin, as in other tropical forests around the globe. Be it through the lens of scarcity of resources and the impossibility of surplus production (Meggers, 1954), or through the lens of abundance and the lack of imperative for it (Neves and Heckenberger, 2019), food storage was a neglected issue for

the study of pre-Columbian Amazonian societies. The presence of buried breads and the new data on archaeological Indigenous bread in the past demonstrate the existence of complex technologies permitting the conservation and storage of foods during long periods, even in the high organic matter and humidity of tropical soils. It opens some avenues for reviewing the role of ingredients used through different technologies of processing, highlighting the importance of fermentation, smoking, and burying as techniques toward improving food durability. It also corroborates recent approaches on mobility patterns and a review of its reduction to nomadism or settlement (Neves and Heckenberger, 2019; Costa, 2009; Da Cunha, 2019; Shiratori et al., 2021). The bread can be understood as a locus of the connection between agriculture and forest management, as it is a product of both cultivated and non-cultivated plants (Cangussu et al., 2021) and can connect paths of dwelling areas with management or trails (Furquim, 2024; Cangussu et al., 2021). It integrates enduring foodscapes (Cassino et al., 2021) in the forest and acts as a timeless link to the present.

Data availability statement

The original contributions presented in the study are included in the article/Supplementary material, further inquiries can be directed to the corresponding author.

Author contributions

KB: Investigation, Writing – original draft, Methodology, Conceptualization, Data curation, Writing – review & editing. LF: Investigation, Writing – original draft, Conceptualization, Data curation, Methodology, Writing – review & editing, Project administration. DC: Conceptualization, Writing – review & editing. AS: Methodology, Writing – review & editing, Resources. GM: Conceptualization, Writing – review & editing. EN: Project administration, Writing – review & editing, Resources. XV: Investigation, Methodology, Supervision, Writing – review & editing.

Funding

The author(s) declare that financial support was received for the research and/or publication of this article. We would like to thank the financial support of the São Paulo Research Foundation (FAPESP, Brazil) to KB (2019/14180-7 and 2022/09459-5), LF (2018/26679-3 and 2022/05776-6), EN (2019/07704-9), XV (2015/19405-6), AS (2017/16451-2), DC (CNPQ 441320/2020-1), and GM (FAPEAM 013/2022). Special thanks to the Alexander Von Humboldt Foundation for supporting the Microarchaeology laboratory at MAE/USP.

Conflict of interest

The authors declare that the research was conducted in the absence of any commercial or financial relationships that could be construed as a potential conflict of interest.

The handling editor CM declared a past collaboration with the authors.

Generative AI statement

The author(s) declare that no Gen AI was used in the creation of this manuscript.

Any alternative text (alt text) provided alongside figures in this article has been generated by Frontiers with the support of artificial intelligence and reasonable efforts have been made to ensure accuracy, including review by the authors wherever possible. If you identify any issues, please contact us.

Publisher's note

Supplementary material

The Supplementary Material for this article can be found online at: https://www.frontiersin.org/articles/10.3389/fearc.2025.1631639/full#supplementary-material

References

Abdullah, A. H. D., Chalimah, S., Primadona, I., and Hanantyo, M. H. G. (2018). "Physical and chemical properties of corn, cassava, and potato starchs," in *IOP Conference Series: Earth and Environmental Science* (Bristol: Institute of Physics Publishing), 1–6.

Adams, F. (1886). *The Genuine Works of Hippocrates*, Vol. 1. New York: W. Wood.

Aguiar, I. J. A., and de Sousa, M. A. (1981). Polyporus indiganus - nova espécie da Amazônia. *Acta Amaz.* 11, 449–55. doi: 10.1590/1809-43921981113449

Arranz-Otaegui, A., Carretero, L. G., Ramsey, M. N., Fuller, D. Q., and Richter, T. (2018). Archaeobotanical evidence reveals the origins of bread 14,400 years ago in northeastern Jordan. *Proc. Natl. Acad. Sci. U.S.A.* 115, 7925–30. doi: 10.1073/pnas.1801071115

Babot, A., Lund, J., and Olmos, V. (2014). Taphonomy in the kitchen: culinary practices and processing residues of native tuberous plants of the south-central Andes. *Intersecc. Antropol.* 15, 35–53.

Babot, P. (2003). "Starch grain damage as an indicator of food processing," in *Phytolith and Starch Research in the Australian-Pacific-Asian: the State of the Art*, eds. D. M. Hart and L. A. Wallis (Canberra: The Australian National University), 69–81.

Barghini, A. (2020). Ethnohistoric review of amylolytic fermentation in Amazonia. *Bol. Mus. Para. Emilio. Goeldi Cien. Hum.* 15–2, 1–23. doi: 10.1590/2178-2547-bgoeldi-2019-0073

Barghini, A. (2022). New data on amylolytic fermentation in the Amazon. *Bol. Mus. Para. Emilio. Goeldi Cien. Hum.* 17, 1–16. doi: 10.1590/2178-2547-bgoeldi-2020-0116

Berna, F., Behar, A., Shahack-Gross, R., Berg, J., Boaretto, E., Gilboa, A., et al. (2007). Sediments exposed to high temperatures: reconstructing pyrotechnological processes in Late Bronze and Iron Age Strata at Tel Dor (Israel). *J. Archaeol. Sci.* 34, 358–73. doi: 10.1016/j.jas.2006.05.011

Bullock, P., Fedoroff, N., Jongerius, A., Stoops, G., Tursina, T., Babel, U., et al. (1985). *Handbook for Soil Thin Sextion Description,* 1st Edn, Vol. 1. London: International Spciety of Soil Science, p. 1–150.

Cangussu, D., Shiratori, K., and Furquim, L. (2021). Notas botánicas sobre aislamiento y contacto. Plantas y vestigios hi-merimã (río Purús/ Amazonía brasileña). *Anthropologica* 39, 339–376. doi: 10.18800/anthropologica.202102.014

Cassino, M. F., Shock, M. P., Furquim, L. P., Ortega, D. D., Machado, J. S., Madella, M., et al. (2021). "Archaeobotany of Brazilian indigenous peoples and their food plants," in *Local Food Plants of Brazil,* eds. M. C. M. Jacob and U. P. Albuquerque (Switzerland: Springer International Publishing), 127–159.

Chisenga, S. M., Workneh, T. S., Bultosa, G., and Alimi, B. A. (2019). Progress in research and applications of cassava flour and starch: a review. *J. Food Sci. Technol.* 56, 2799–813. doi: 10.1007/s13197-019-03814-6

Clark, J. D. (2001). "Appendix B geophagy and Kalambo falls clays," in *Kalambo Falls Prehistoric Site III—The Earlier Cultures: Middle and Earlier Stone Age*. Cambridge: Cambridge University Press, 659–664.

Clement, C. R., Denevan, W. M., Heckenberger, M. J., Junqueira, A. B., Neves, E. G., Teixeira, W. G., et al. (2015). The domestication of amazonia before european conquest. *Proc. R Soc. B Biol. Sci.* 282, 1–9. doi: 10.1098/rspb.2015.0813

Costa, L. (2009). Worthless movement: agricultural regression and mobility. *Tipití J. Soc. Anthropol. Lowl. South Am.* 7, 151–180. doi: 10.70845/2572-3626.1106

Crosby, A. W. (2003). *The Columbian Exchange Biological and Cultural Consequences of 1492,* 30th Anniversary Edition. London: Bloomsbury Academic.

Da Cunha, M. C. (2019). Antidomestication in the amazon: swidden and its foes. *HAU J. Ethnogr. Theory.* 9, 126–36. doi: 10.1086/703870

da Silva Araujo, I. J., and de Sousa, M. A. (1978). Nota prévia sobre o pão do índio da Amazônia Brasileira. *Acta Amaz.* 8, 316–316. doi: 10.1590/1809-43921978082316

de Oliveira, J. C. (2012). Entre plantas e palavras: modos de constituição de saberes entre os Wajãpi (AP). São Paulo: Universidade de São Paulo.

den Steinen, K. V. (1940). *Entre os aborígenes do Brasil Central*, Vol. XXXIV a LVIII. São Paulo: Revista do Arquivo - Departamento de cultura, 749.

Diabor, E., Funkenbusch, P., and Kaufmann, E. E. (2019). Characterization of cassava fiber of different genotypes as a potential reinforcement biomaterial for possible tissue engineering composite scaffold application. *Fibers Polym.* 20, 217–28. doi: 10.1007/s12221-019-8702-9

dos Santos, G. M., Cangussu, D., Furquim, L. P., Watling, J., and Neves, E. G. (2021). Indigenous bread and vegetable pulp: bonds between past and present in indigenous Amazon. *Bol. Mus. Para. Emilio Goeldi Cien. Hum.* 16, 1–20. doi: 10.1590/2178-2547-bgoeldi-2020-0012

Feniman, C. M. (2004). *Caracterização de raízes de mandioca (manihot esculenta crantz) do cultivar iac 576-70 quanto à cocção, composição química e propriedades do amido em duas épocas de colheita.* Piracicaba. ESALQ.

Fernandes, E. (1950). Medicina e maneiras de tratamentos entre os índios Pariukur (Aruak). *Am. Indig.* X, 309–320.

Figueiredo, P. G., de Moraes-Dallaqua M. A., Bicudo, S. J., Tanamati, F Y., and Aguiar, E. B. (2015). Development of tuberous cassava roots under different tillage systems: descriptive anatomy. *Plant Prod. Sci.* 18, 241–245. doi: 10.1626/pps.18.241

Fitzpatrick, E. A. (1984). *Micromorphology of Soils,* 1st Edn. London and New York: Springer Netherlands, 449.

Fornari Junior, C. C. M. (2017). *Fibras vegetais para compósitos poliméricos*. Ilhéus, BA: Editus.

França, L. (2024). Before, we didn't eat manioc flour": historical and social transformations in food techniques among Indigenous Peoples of the Rio Negro basin in the Brazilian Amazon. *Tipití J. Soc. Anthropol. Lowl. South Am.* 20, 256–73. doi: 10.70845/2572-3626.1407

França, L., and Fontes, F. (2022). Alimentação na floresta: relações entre frutos, comidas e os yóopinai entre os Baniwa, Alto Rio Negro. *Maloca Rev. Estud. Indígenas* 5, 1–36. doi: 10.20396/MALOCA.V5I00.15822

Furquim, L. (2024). *Dos Roçados às Panelas: Alimentação e Cultivo na Amazônia Antiga*. São Paulo: Museu de arqueologia e Etnologia - USP.

Gumilla, J. (1745). *El Orinoco ilustrado, y defendido, história natural, civil, y geographica de este gran rio, y de sus caudalosas vertientes*, Vol. 1. Madrid: Companhia de Jesus, p. 472.

Henry, A. G., Hudson, H. F., and Piperno, D. R. (2008). Changes in starch grain morphologies from cooking. *J. Archaeol. Sci.* 36, 915–22. doi: 10.1016/j.jas.2008.11.008

Humphreys, A. M., Govaerts, R., Ficinski, S. Z., Nic Lughadha, E., and Vorontsova, M. S. (2019). Global dataset shows geography and life form predict modern plant extinction and rediscovery. *Nat. Ecol. Evol.* 3, 1043–1047. doi: 10.1038/s41559-019-0906-2

Ibrahim, S., Daik, R., and Abdullah, I. (2014). Functionalization of liquid natural rubber via oxidative degradation of natural rubber. *Polymers* 6, 2928–41. doi: 10.3390/polym6122928

Kaxuyana, N. I. W., Girardi, L. G., and Jácome, C. P. (2024). "Imagens do tempo: materialidade, temporalidade e territorialidade na retomada Kahyana e Katxuyana," in *Arqueologias históricas nos rios Tapajós, Trombetas e amazonas*, 276–304. Santarém. ed. Appris.

Krahô, M. C., Krahô, D. P., Moreira, L., Dias, T. A. B., de Cerqueira Zarur, S. B. B., Bueno, Y. M. (2005). *A Preparação do Paparuto-Povo Indígena Krahô*. Available online at: https://www.infoteca.cnptia.embrapa.br/bitstream/doc/570879/1/doc146.pdf (Accessed December 10, 2024).

Lacerda, L. G., Almeida, R. R., Demiate, I. M., Carvalho Filho, M. A. S., Vasconcelos, E. C., Woiciechowski, A. L., et al. (2009). Thermoanalytical and starch content evaluation of cassava bagasse as agro-industrial residue. *Braz. Arch. Biol. Technol.* 52, 143–50. doi: 10.1590/S1516-89132009000700019

Laufer, B. (1930). Geophagy. *Anthropol. Series* XVIII, 101–94. doi: 10.5962/bhl.title.3396

Levis, C., Costa, F. R. C., Bongers, F., Peña-Claros, M., Clement, C. R., Junqueira, A. B., et al. (2017). Persistent effects of pre-Columbian plant domestication on Amazonian forest composition. *Science* 355, 925–31. doi: 10.1126/science.aal0157

Levis, C., Flores, B. M., Moreira, P. A., Luize, B. G., Alves, R. P., Franco-Moraes, J., et al. (2018). How people domesticated Amazonian forests. *Front. Ecol. Evol.* 5, 1–20. doi: 10.3389/fevo.2017.00171

Meggers, B. J. (1954). Environmental limitation on the development of culture. *Am. Anthropol.* 56, 801–824. doi: 10.1525/aa.1954.56.5.02a00060

Navia, D. P., and Villada, H. S. (2012). "Thermoplastic cassava flour," in *Thermoplastic Elastomers*, ed. A. Z. El-Sonbati (Rijeka: InTech), 23–38.

Neves, E. G., and Heckenberger, M. J. (2019). The call of the wild: rethinking food production in ancient Amazonia. *Annu. Rev. Anthropol.* 48, 371–388. doi: 10.1146/annurev-anthro-102218-011057

Paes, S. S., Yakimets, I., and Mitchell, J. R. (2008). Influence of gelatinization process on functional properties of cassava starch films. *Food Hydrocoll.* 22, 788–97. doi: 10.1016/j.foodhyd.2007.03.008

Paulo, S. (2019). *Outros Pioneiros do Sudoeste Amazônico: Ocupações Holocênicas na Bacia do Alto Rio Madeira*. Guilherme Zdonek Mongeló Guilherme Zdonek Mongeló Outros Pioneiros do Sudoeste Amazônico: Ocupações Holocênicas na Bacia do Alto Rio Madeira.

Pereira, L. T., Sulzbacher, M. A., and Baltazar, J. M. (2018). "Diversidade De Fungos Brasileiros E Alimentação: O Que Podemos Consumir?," in *III Fórum Ambient Angatuba* (Angatuba, SP: Resumo Expand nos An do III Fórum Ambient).

Perrone-Moisés, B. (2015). *Festa e Guerra*. São Paulo: Universidade de São Paulo.

Putzke, J., da Silva Santos, A. B., Castro, R. M., and Putzke, M. (2021). Macroscopy fungi used people in Brazil: a review of and perspectives on the cultivation of edible species. *Agric. Fam. Pesqui Formação Desenvolv.* 15, 87–109. doi: 10.18542/raf.v15i2.9839

Qi, M., Song, J., Jiang, L., Li, L., Xu, M., Li, Y., et al. (2024). Understanding the degradation mechanisms of cyanide and starch in cassava flour during extrusion processing. *Innov. Food Sci. Emerg. Technol.* 91:103548. doi: 10.1016/j.ifset.2023.103548

Quinn, P. (2013). *Ceramic Petrography*. Oxford: Archeopress.

Quinn, P. S. (2022). *Thin Section Petrography, Geochemistry and Scanning Electron Microscopy of Archaeological Ceramics*, 1st Edn. Oxford: Archaeopress, 2–466.

Rolere, S., Liengprayoon, S., Vaysse, L., Sainte-Beuve, J., and Bonfils, F. (2015). Investigating natural rubber composition with Fourier Transform Infrared (FT-IR) spectroscopy: a rapid and non-destructive method to determine both protein and lipid contents simultaneously. *Polym. Test.* 43, 83–93. doi: 10.1016/j.polymertesting.2015.02.011

Santos, C. A., da Silva, F. E. C., da Silva, S. F. S. M., Sullasi, H. L., de Paula, A. S., Oliveira, C. A., et al. (2014). O pão do índio dos Nukini da Amazônia: estudo de caso sobre o uso de suprimentos específicos na dieta alimentar indígena. *Fundação Mus do Homem Am.* 1, 58–77.

Sanuma, O. I., Tokimoto, K., Sanuma, C., Autuori, J., Sanuma, L. R., Sanuma, M., et al. (2018). *Enciclopédia dos Alimentos Yanomami (Sanöma).* São Paulo: Instituto Socioambiental, p. 108.

Shiratori, K., Cangussu, D., and Pereira Furquim, L. (2021). Life in three scenarios: plant controversies between Jamamadi gardens and Hi-Merimã patauá palm orchards (Middle Purus River, Amazonas, Brazil). *J. Anthropol. Archaeol.* 64:101358. doi: 10.1016/j.jaa.2021.101358

Simões, M. F. (1981). As pesuisas arqueológicas no Museu Paraense Emilio Goeldi. *Acta Amazônica* 11, 149–65. doi: 10.1590/1809-43921981111s149

Spix e Martius (2017). *Viagem pelo Brasil (1817-1820),* Vol. III. Brasília: Senado Federal, 1–492.

Stokes, F. J., Benites, S., Ekman, A., Suruí, U. A., Furquim, L., Winkelmann, R., et al. (2025). Tropical deforestation and indigenous resistance over the longue durée in South America. *J. Glob. Hist.* 20, 1–22. doi: 10.1017/S1740022825000051

Stoops, G. (2021). Guidelines for Analysis and Description of Soil and Regolith Thin Sections, Vols. 1–231. Hobokkem: Wiley-ACSESS.

Teodoro, A. P., Mali, S., Romero, N., and de Carvalho, G. M. (2015). Cassava starch films containing acetylated starch nanoparticles as reinforcement: physical and mechanical characterization. *Carbohydr. Polym*. 126, 9–16. doi: 10.1016/j.carbpol.2015.03.021

Versino, F., and García, M. A. (2014). Cassava (*Manihot esculenta*) starch films reinforced with natural fibrous filler. *Ind. Crops Prod*. 58, 305–14. doi: 10.1016/j.indcrop.2014.04.040

Villagran, X. S., Strauss, A., Alves, M., and Oliveira, R. E. (2019). Virtual micromorphology: the application of micro-CT scanning for the identification of termite mounds in archaeological sediments. *J. Archaeol. Sci. Rep*. 24, 785–95. doi: 10.1016/j.jasrep.2019.02.035

Villagran, X. S., Strauss, A., Miller, C., Ligouis, B., and Oliveira, R. (2017). Buried in ashes: site formation processes at Lapa do Santo rockshelter, east-central Brazil. *J. Archaeol. Sci*. 77, 10–34. doi: 10.1016/j.jas.2016.07.008

Von Humboldt, A., and Bonpland, A. (1852). *Personal Narrative of Travels to the Equinoctial Regions of America, During the Years 1799–1804. Vol. 1–3*. London: Henry G. Bohn.

Weiner, S. (2010). *Microarchaeology: Beyond the Visible Archaeological Record*. Cambridge: Cambridge University Press.